# Findings Report

## Collaborative Research: Plankton Community Structure and Iron Distribution in the Southern Drake Passage and Scotia Sea

**B. Greg Mitchell, Farooq Azam, Katherine Barbeau, Sarah Gille, Osmund Holm-Hansen**
**Awardee: Scripps Institution of Oceanography Award Number: ANT 04-44134**

### Background

The Southern Ocean is the largest oceanic area with a high inventory of inorganic macro-nutrients and relatively low phytoplankton chlorophyll (HNLC; Chisholm and Morel 1991). The paradox of why phytoplankton biomass is generally so low in Antarctic waters during summer challenged researchers for decades (Hart, 1942; Holm-Hansen, 1985; El-Sayed 1987). Reports of very low Fe concentrations and Fe enrichment experiments (*in vitro* and *in situ*) indicate that iron often limits phytoplankton biomass in the Southern Ocean (Martin et al, 1990a; 1990b; Nolting et al., 1991; deBaar et al., 1990; Holm-Hansen et al., 1994; Löscher et al., 1997; Sedwick and DiTullio, 1997; Takeda, 1998; Sedwick et al., 1999; Boyd et al., 2000; Strutton et al., 2000; Fitzwater et al., 2000; Smetacek, 2001; Boyd 2002 and 2004; Buesseler et al. 2003; Coale et al., 2004; Buesseler et al., 2004). Variations in iron supply may govern Southern Ocean carbon export during glacial-interglacial cycles (Martin, 1990). For the contemporary Southern Ocean, significant questions remain regarding how variable supply of iron regulates spatial and temporal distributions of plankton, plankton community structure and ecology, and the sequestration of $CO_2$ to the ocean interior via the biological pump.

### Drake Passage Plankton Community Transition

Global and regional analyses of satellite data have led to our discovery of a major plankton community transition associated with bathymetry in the Drake Passage. Figure 1A illustrates the strong regional contrasts in Southern Ocean surface chl-a during January. Two massive Blue Water Zones (BWZ; Pacific and Indian Ocean sectors) south of the Polar Front and north of the ice edge during summer comprise approximately 30% of the Southern Ocean (Holm-Hansen et al. 2005). The BWZ in the Indian Ocean sector ends at the Kerguelen Shelf and the BWZ in the Pacific Sector ends in the Southern Drake Passage, near the very low iron station originally reported by Martin et al. (1990). A predictable front in chl-a is found in late summer near the Shackleton Transverse Ridge (STR), a 500 km ridge within the Shackleton Fracture Zone (SFZ) that rises from a basin greater than 4000 m depth to less than 1000 m in the southern Drake Passage (Figure 2A ). The location of the very low iron ACC station reported by Martin et al. (1990) is shown in Figure 2B, just west of the STR at the western end of the south Pacific sector BWZ. Our research has focused on the transition east of that station by Martin, where low chl-a water from the south Pacific sector of the Antarctic Circumpolar Current (ACC) is rapidly transformed as it flows from the southern Drake Passage into the Scotia Sea.

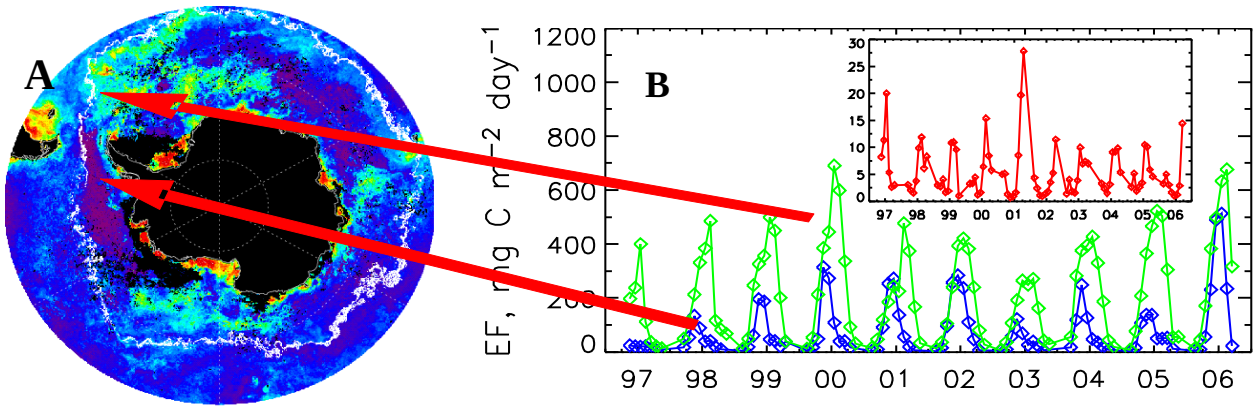


**Figure 1**. **A.** Mean surface chl-a concentrations obtained from a SeaWiFS composite of January (1998/1999). The white line represents the Antarctic Polar Front (PF) defined as the 4°C frontal region determined from the January 1998 monthly composite satellite sea surface temperature (NASA AVHRR Pathfinder). A dramatic plankton ecosystem transition occurs at the Shackleton Fracture Zone in the Drake Passage. **B.** 10-year time-series of "Export Flux" (EF) of organic carbon from the photic zone based on monthly satellite composites for the regions east and west of the SFZ indicated by arrows, respectively. In **B.** green lines correspond to the high chlorophyll water east of SFZ, and the blue lines correspond to the low chlorophyll, iron poor water, west of SFZ. The inset (red line) is the 10-year time-series of the ratio of EF east of SFZ divided by EF west of SFZ. The regions were defined as follows: northern and southern boundaries are climatological Polar Front (PF) and Southern Boundary (SB) specified by Orsi et al. (1995). The SFZ separates the east and west domains. The total area between SFZ and the arc defined by South Georgia and South Sandwich Islands and bounded north and south by the PF and SB, respectively, is used for the eastern domain. The domain west of SFZ comprises the same total area as the eastern domain, and also is bounded north and south by the PF and SB.

Figure 1B shows a time series of Export Flux from the photic zone (EF) for the regions east and west of the STR using satellite-derived chl-a, temperature and surface irradiance as input to the model of Laws et al. (2000) and Laws (2004). The region east of STR has higher values of EF, and there are strong seasonal and interannual variations that may be due in part to the mass transport of coastal shelf iron into the southern Scotia Sea. For example, in the Southern Scotia Sea values of EF for the austral summer peaks for 1999-2000 and 2005-2006 are more than double the values estimated for the 2002-2003 peaks. The source of this variability is not known, but has very significant implications for carbon cycle dynamics as well as sustainability of higher trophic levels that depend on the plankton ecosystem.

Results from our NSF-funded cruises during austral summer 2004 (LMG0402) and winter (NBP0606) indicate that interaction of the Southern ACC Front (SACCF) with topography in the region of the STR results in transport of iron-rich shelf-modified water offshore to fertilize the waters of the Southern Drake Passage and Scotia Sea. This study area, with its reproducible and strong chl-a gradients, provides an ideal location to study natural iron fertilization processes to improve our ability to predict how Southern Ocean export production might be affected by climate change. We have carried out an interdisciplinary program with cooperation with the NOAA Antarctic Marine Living Resources program. Separate NASA funding provided complimentary satellite data analysis for ocean biology and ocean physics.

**Hypotheses**

***Hypothesis 1. Flow of major surface currents including the Southern ACC Front and the Weddell Sea outflow are iron enriched though shelf mixing processes north of Elephant Island and west of South Orkney Islands before flowing northeast into the Scotia Sea. The volume transport of the SACCF through the Shackleton Gap determines the off-shelf transport of iron-rich shelf water.***

***Hypothesis 2. Iron enrichment creates strong gradients in plankton community structure in the vicinity of the STR, and the community evolves with time as it is transported east. As the community ages, export production is elevated and the physiological ecology of phytoplankton and bacteria responds to depletion of the natural iron fertilization.***

**Overview**

This findings report for NSF Award ANT 04-44134 is submitted by the Scripps Institution of Oceanography (SIO), lead institution for our Collaborative Research project. See Table 1 for details of participating Principal Investigators and their roles in the project. Separate annual reports submitted by the principal investigators at collaborative institutions include:

Matthew Charette, Woods Hole Oceanographic Institute, NSF Award ANT04-43869

Christopher Measures, University of Hawaii, NSF Award ANT 04-43403

Meng Zhou, University of Massachusetts, Boston, NSF Award ANT 04-44040.

**Table 1. Summary of main observations made, and the responsible investigator(s).**

| Analysis | Investigator(s) | Publications |
|---|---|---|
| **Biology and Optics** | | |
| Phytoplankton production and physiology (PvsE) | Mitchell, Holm-Hansen | 15-18, 20, 21, 24-26, 32 |
| Phytoplankton community composition | Hewes, Mitchell, Selph | 14, 19, 29, 30 |
| Active Fluorescence (FRRF), Optics | Mitchell | 15, 16, 24-26, 32 |
| Biomass (chl-a, HPLC, POC/PON) | Holm-Hansen, Mitchell, Hewes | 13, 16, 17, 23, 24 |
| Bacterioplankton, microheterotrophs | Azam, Hewes, Selph | 22 |
| Zooplankton acoustic backscatter/samples | Zhou | |
| Phytoplankton growth experiments | Barbeau, Azam, Hewes, Holm-Hansen, Mitchell, Selph | 19, 29 |
| **Physical Environment** | | |
| ADCP, hydrography, drifters, mixing | Zhou, Gille | 12-14, 33-36 |
| **Chemistry** | | |
| Trace metals Fe, Al, Mn | Measures, Barbeau | 3, 7, 19 |
| Macronutrients, N, P, Si | Mitchell, Hewes, Holm-Hansen | 14, 17, 18, 29 |
| Th, Ra, Export Flux | Charette | 1, 4-6, 8, 10, 17, 26, 27, 31 |
| **Satellite Analysis (Separate NASA funding)** | | |
| Chl, sea surface temperature (SST | Mitchell, Kahru | 21 |
| Eddy energy, surface velocities, winds) | Gille | 20, 21 |


1. Allen, J. D., et al., (2006)
2. Allison, D., (2006)
3. Barbeau, K., et al, (2006)
4. Bourquin M., et al., (2007), submitted.*
5. Bourquin M., et al., (2007)
6. Bourquin M.et al., (2006)
7. Buck, K.N., et al., (2008)
8. Charette, M.A.,et al., (2007), in press*.
9. Dorland, et al., 2007, revised*
10. Dulaiova, H.; et al. (2007)
11. Elipot, S and Gille, S (2006)
12. Frants, M., (2006)
13. Frants, M., et al., (2007)
14. Hewes, C. D., et al., accepted.*
15. Hiscock, M., et al, submitted*
16. Hiscock, M., et al., (2007)
17. Holm-Hansen, O., et al., (2005) *
18. Holm-Hansen, O., et al., (2006)
19. Hopkinson, et al., (2007)*
20. Kahru, M., and B.G. Mitchell, (2006)
21. Kahru, M., et al. (2007).*
22. Malfatti, F., et al., (2005)
23. Measures, C., et al. (2006), submitted*
24. Mitchell B.G., et al., (2007)
25. Mitchell, B.G., et al., (2006)
26. Moisan, T. and Mitchell, B., submitted*
27. Planquette, H., et al. (2007), submitted.*
28. Planquette, H., et al., (2007)
29. Selph, K., et al., (2005)
30. Selph, K., et al. (2006
31. van Beek P., et al., (2007) in revision.*
32. Wang, H., et al., (2006)
33. Zhou, M., et al, (2006)*
34. Zhou, M., et al., (2006), in revision *
35. Zhou, M.,et al, (2006)
36. Zhou, et al., (2007) submitted.*


*** peer reviewed journal articles**

During our summer 2004 cruise on RV L. M. Gould (LMG0402) our Collaborative Research group performed the first cruise to establish the linkage between chl and Fe gradients in the Southern Scotia Sea focusing on the STR in the Southern Drake Passage. Our region of focus was guided by our findings from extensive satellite analyses that indicated a major transition in phytoplankton productivity at the STR (Holm-Hansen et al., 2006; Kahru et al., 2007). In summer 2006 the SIO and WHOI team members returned on the NOAA AMLR cruise to document the large gradient in export flux concurrent with this phenomenon, and to develop models relating net primary production (NPP) to export flux (EF). During July – August 2006 the full team of 4 institutions executed a winter cruise on Nathaniel B. Palmer (NBP0606). The iron-related biogeochemical transition which we have documented in the Southern Drake Passage is a microcosm of the major biogeochemical transition which occurs between the massive Blue Water Zone in the Pacific Sector of the Southern Ocean and the highly productive waters of the Scotia Sea to the east of the Antarctic Peninsula (see Figure 1). Analysis of our drifter tracks and historic hydrographic data indicate that the flow from the region we studied near the STR and the Elephant Island shelf remains bounded by the ACC Polar Front (ACCPF) to the north and the ACC Southern Boundary (ACCSB) to the south with the Southern ACC Front (SACCF). As we summarize in more detail below, and in the findings reports of our Collaborative Institutions, the water between the ACCPF and ACCSB has been enriched with shelf-derived iron by the mixing processes we have discovered and this iron enrichment contributes to the high productivity throughout the Southern Scotia Sea.

Since ours is an interdisciplinary project, findings by our collaborators at others institutions are fundamental to the work and findings by the SIO investigators. For many elements of our project, members of different institutions collaborated on data processing and analysis. Details of findings of our collaborators are included in their separate reports, but some aspects of those findings are also summarized here in the context of our interdisciplinary analyses and interpretation of the results of the SIO team. The main observations, investigators responsible, and publications resulting from our work are summarized in Table 1.

**Physical Oceanography**

An accurate description of water masses and their regional circulation is required to understand if shelf-modified waters contribute to the observed transitions in plankton communities as the ASCC flows past the STR. The focus of this study is the Southern Drake Passage region on both sides of the STR and the southern Scotia Sea (Figure 2). Prevailing ocean transport in the Drake Passage is from the west or southwest where the ocean depth is generally greater than 4000 m. During our February-March 2004 cruise, the low chl-a, low iron ACC water from the Pacific sector BWZ flowed southeastward parallel to the STR at up to 50 cm $s^{-1}$. The flow was up to 100 cm $s^{-1}$ as this branch of the ACC associated with the SACCF passed the narrow Shackleton Gap - a 3000 m deep break between the STR and the Elephant Island shelf (Figure 2). After passing the Shackleton Gap, the majority of this jet was steered northward along the east side of STR re-joining the main ACC at 59$^{o}$S where it was steered east by the West Scotia Ridge. On the northern shelf break of Elephant Island, a branch of the ACC water flowed eastward over Shackleton Bank toward the South Scotia Ridge. See Figure 2A for bathymetry features in our study region.

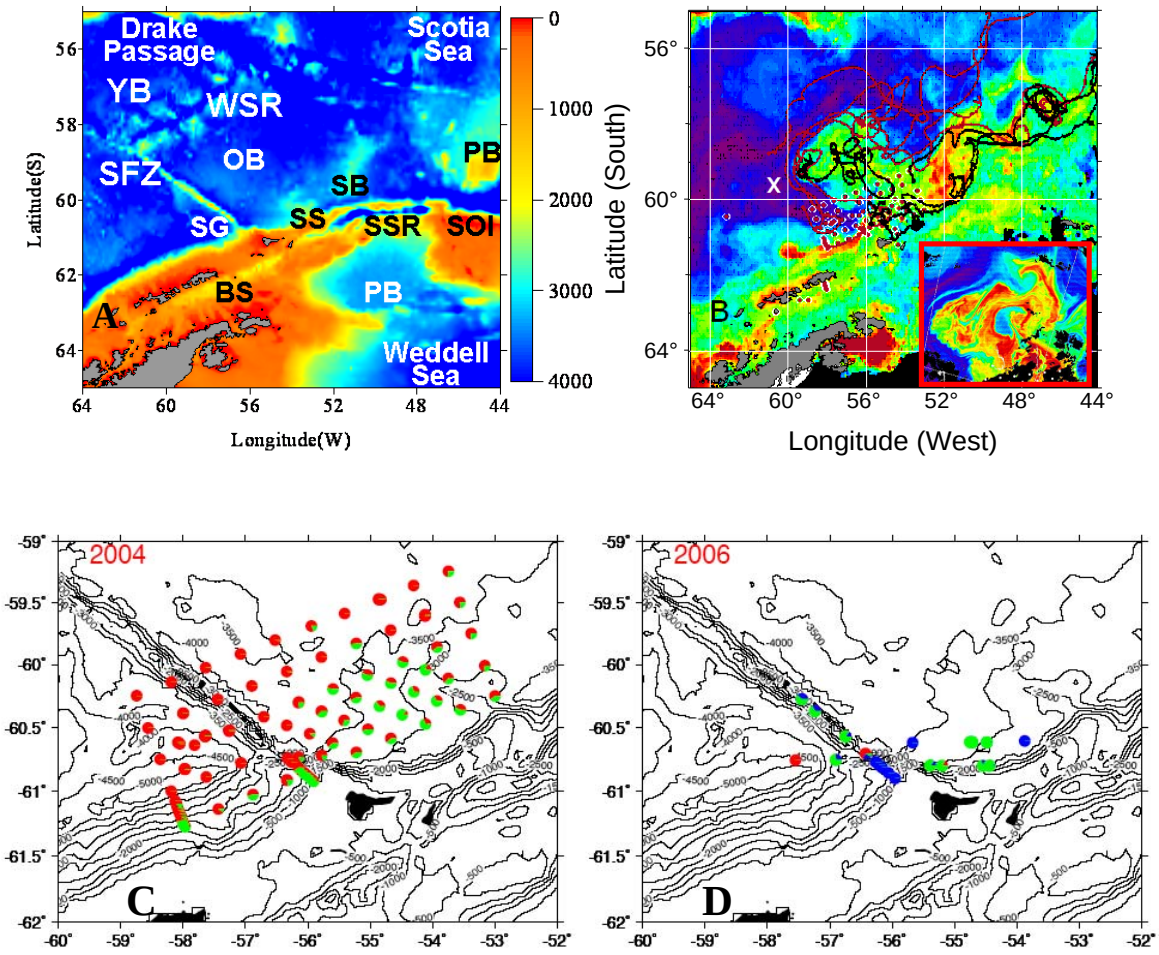


**Figure 2. A .** Bathymetry of the Southern Drake Passage and Southern Scotia Sea. Abbreviations are defined as: BS=Bransfield Strait, EI=Elephant Island, OB=Ona Basin, PB=Pirie Bank, SB=Shackleton Bank, SFZ=Shackleton Fracture Zone, SG=Shackleton Gap, SOI=South Orkney Islands, SS=Shackleton Shelf, SSI=South Shetland Islands, SSR=South Scotia Ridge, WSR=West Scotia Ridge, and YB=Yaghan Basin. **B**. MODIS chl-a composite for February 2004 with selected Lagrangian surface drifter tracks, and the station grid of our 2004 cruise on the R/V Gould. The inset on lower right is the MODIS unmapped high resolution image over the Ona Basin for March 19, 2004 showing dramatic evidence of water mass mixing over this deep basin. The white **X** indicates the location of the low Fe station reported by Martin et al. (1990). **C.** Detailed map of the LMG 0402 survey stations. During LMG0402 three high resolution surveys across the shelf break (two north and one south into Bransfield Strait), were accomplished to resolve shelf-intensified currents and to explore mechanisms that govern the mixing processes between iron rich shelf water and iron poor ACC water. **D.** Station locations during NBP0606 in the region north of the Elephant Island Shelf. We also carried out a survey southeast of the map into the Powel Basin of the Weddell Sea, and South of King George Island across the Bransfield Strait. Harsh weather conditions during winter prevented completion of a detailed survey similar to LMG0402.

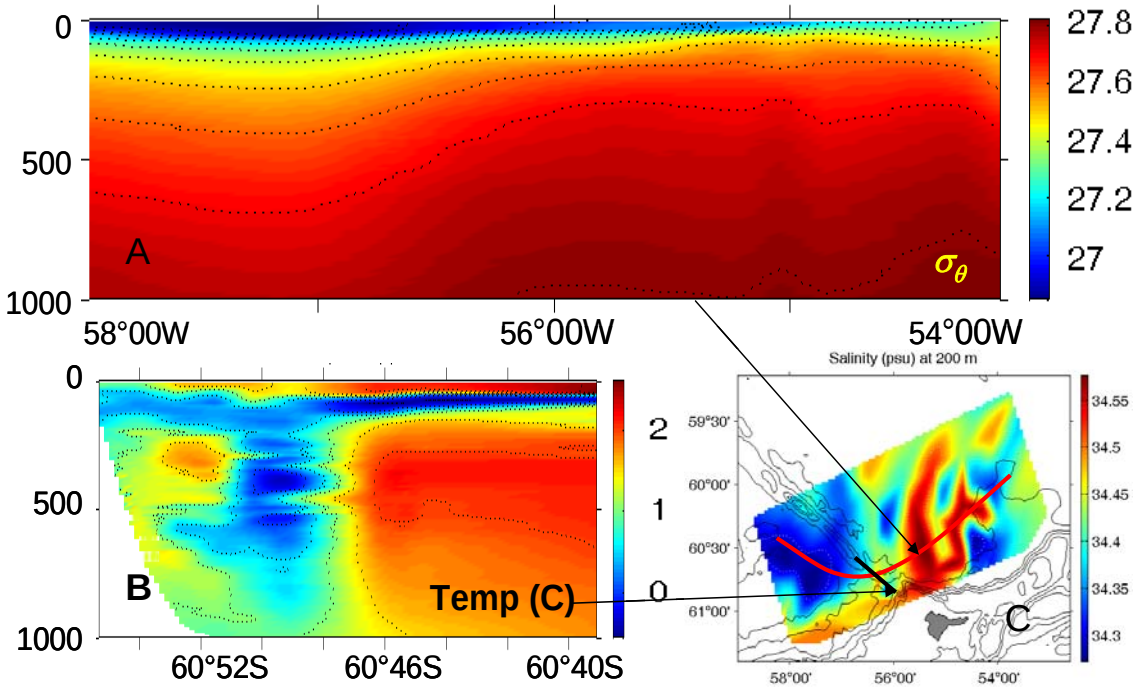


**Figure 3**. **A.** The potential density transect from the ACC to the Shackleton Bank (SB), indicated by the red solid line in **3C**. **B.** High resolution (2-3 km ) temperature transect crossing the Shackleton Gap, indicated by the black solid line in **3C. C.** The salinity field at 200 m for our LMG 0402 survey.

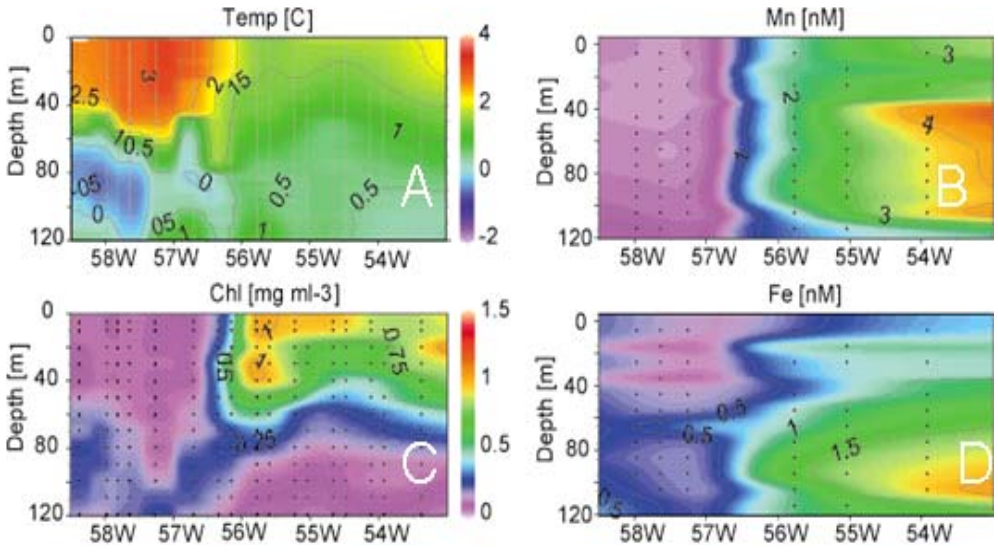


**Figure 4**. Vertical sections of temperature (**A**), manganese (**B**), chlorophyll-a (**C**) and iron (**D**) for stations along a transect from ACC water to the Shackleton Bank (SB). The station positions were located along the red line shown in Figure **3C**.

The trajectories of Lagrangian drifters released very close together within the Shackleton Gap followed either the main SACCF northward in parallel to the STR, or the along-shelf path (red and black drifter trajectories, respectively in Figure 2B). A 2-3 km high-resolution hydrographic transect crossing the Gap revealed that the front separating the ACC and shelf waters was deeper than 1000 m within 2-3 km (Figure 3B). Interleaving waters in the frontal zone were indicative of horizontal mixing processes. The ACC water flowing east along the Elephant Island shelf and Shackleton Shelf lost momentum, and the deep water rose up to 200 m, a significant increase in the potential energy (Figure 3A). The ACC intrusion on the Shackleton Shelf was evident from the high salinity tongue at 200 m (Figure 3C). The intrusion of ACC water onto the shelf pushes cold water off the shelf and appears to drive mixing processes.

East of the STR within the Ona Basin, mesoscale eddies mix ACC water with shelf water, as indicated by drifter trajectories, T-S characteristics, and sections/surface maps from our survey grid (Zhou et al., 2007; Figures 2, 3, and 4). During summer 2004, waters from both the ACC and Bransfield Strait flowed east along the north and south shelf breaks of South Shetland Islands and Elephant Island, respectively. The Bransfield Current was up to 100 cm $s^{-1}$ south of King George Island. We expect that these two currents continue eastward (Hofmann et al., 1996) and eventually interact with Weddell Sea water flowing north from Powell Basin (Schodlok et al., 2002). We speculate that these three water sources become mixed over the South Scotia Ridge before continuing east in the Scotia Sea. During the NBP0606 winter cruise, a similar flow pattern was found but surface mixed layers were much deeper, especially on the shelf and in the Bransfield Strait.

Optimal MultiParameter (OMP) analysis (Tomczak, 1981; Tomczak and Large, 1989) was used for a quantitative analysis of the mixing of water masses based on a model of linear mixing. The method uses robust statistical methods using input of source water mass properties (e.g. temperature, salinity and dissolved oxygen) to infer the mixing history of a water parcel. OMP analyses (Frants et al. 2007) indicate that ACC and shelf water are the two main sources for mixed waters that support phytoplankton blooms off shore (e.g. Stations 27 and 57 in Figure 5). A relatively small fraction of shelf water (10-20%), mixed with ACC water, supports chlorophyll that is 5-10x higher than the ACC source water.

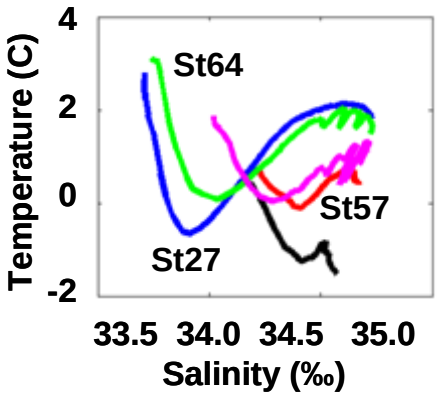


**Figure 5**. T-S diagrams of representative water types found during LMG0402. Water from the mixed layer at these stations was used for controlled iron enrichment experiments summarized in Figures 7 and 8. Water types were: ACC station 27 (Blue), shelf station 57 (Red), and mixed station 64 (Green). Bransfield Strait water is shown in Black and a mixed station located close to the shelf is in Magenta.

## Chemistry

### *Macro-nutrient distribution*

During LMG0402, the mean concentrations of nitrate, ammonia, phosphate, and silicic acid in low chl-a waters (station 27) were 23.6, 0.84, 1.34, and 19.7 μM, respectively; in green waters to the east of the STR (station 64) the concentrations were 24.4, 0.55, 1.37, and 44.7 μM, respectively; and in shelf waters (station 57) the concentrations were 25.1, 0.71, 1.42, and 55.0 μM, respectively. Stations 27, 57 and 64 were detailed process stations during LMG0402 where we carried out all analyses and set up controlled Fe amendment phytoplankton growth experiments. For all LMG0402 stations, concentrations of N, P, and Si were high and considered saturating for phytoplankton growth. However, their relative ratios provide insight into community structure. Under iron limitation, diatoms become more heavily silicified (Hutchins and Bruland, 1998; De La Rocha, 2000). The low silicic acid concentrations in low chl-a ACC waters and the significant drawdown of Si relative to N as measured in our iron-enrichment experiments (see Table 2) may be caused by heavier silicification under iron limitation. Our 2004 data indicate that macronutrient concentrations are similar below ~100m for the entire study grid (Hewes et al., 2007). The relatively high ammonia concentrations in low chl-a ACC waters within the mixed layer is consistent with previous data (Biggs et al. 1982) and may result from the limitation of Fe and changes in the structure and dynamics of the microbial food web.

### *Metals*

Horizontal transport of water from the Antarctic Peninsula shelf could be an important source of iron to regions downstream and off-shelf. To evaluate this possibility, we obtained real-time, high resolution measurements of surface and profiled concentrations of dissolved Fe, Al and Mn (Measures et. al., 1995; Resing and Measures 1994; Resing and Mottl, 1992) to map horizontal and vertical gradients in Fe concentration and their co-variation with water properties (e.g. salinity and temperature) and source indicators (Al and Mn). Absolute abundances and ratios of Fe, Al and Mn were useful in elucidating potential sources of Fe to our study region and providing evidence of mixing between ACC and shelf waters. During LMG0402, dissolved Fe concentrations north of the peninsula shelf ranged by two orders of magnitude from 0.050 to 5.46 nM, dissolved Al varied 15 fold from 0.48 to 7.6 nM, and Mn varied by more than 200-fold from 0.04 to 9 nM. Figure 4 illustrates sections of temperature, chl-a, Mn and Fe along a transect indicated in Figure 3C. Lowest concentrations for all three dissolved trace elements were associated with the blue ACC water west of the STR and highest values were in the coastal shelf stations or in the water advected over Ona Basin. Locations with high concentrations of Mn, a tracer of shelf source water, but low values of Fe were found in the northeast part of our grid, east of STR. These stations are presumed to represent the downstream biogeochemical modification of the enriched shelf waters where Fe has been removed from the dissolved phase into the particulate phytoplankton phase.

During the Southern Ocean Iron Enrichment Experiment (SOIREE) the bloom persisted 42 days after Fe addition (Boyd et al., 2000). Extended blooms were also observed in the Southern Ocean Iron Experiment (SOFEX, Coale et al., 2004). One hypothesis to explain these observations is that phytoplankton may be able to access ligand-bound Fe (Maldonado et. al., 2001). Photoredox

cycling of Fe may also result in the formation of labile Fe(II) (Croot et al., 2001; Barbeau et al. 2001). At selected locations we determined concentrations of Fe(II) using chemiluminescent analysis (FeLume, Waterville Analytical) as well as strong Fe(III)-binding ligands using competitive ligand exchange/adsorptive cathodic stripping voltammetric methods (Croot and Johansson 2000). Ligands and photoredox cycling may contribute to longevity and large spatial extent of observed blooms in the Southern Scotia Sea down-stream from our study region (Kahru et al. 2007; Figure 6).

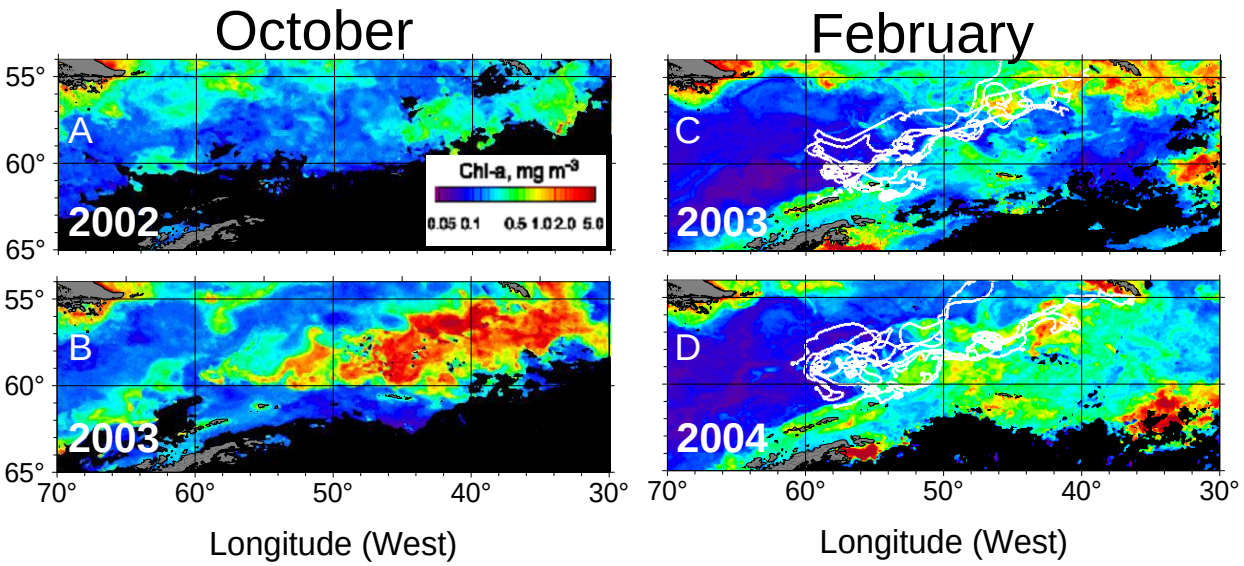


**Figure 6**. MODIS chl-a images of the Drake Passage and Scotia Sea in October 2002 (**A**), October 2003 (**B**), February 2003 (**C**) and February 2004 (**D**). Lagrangian drifters released as part of our multi-agency cooperative effort with the NOAA AMLR and Global Drifter Programs are overlain on the images for the respective year of their release. It is surprising to see such a massive early spring bloom in October, 2003. Strong interannual variability in early spring is hypothesized to be related to the position and strength of the ACC fronts. Persistence of blooms in the Southern Scotia Sea from October through March may be related to binding of Fe by organic ligands, and photoredox cycling of Fe.

SIO analysis of Fe speciation data from LMG0402 indicated that the chlorophyll gradient in southern Drake Passage was accompanied by a strong gradient in organic Fe(III)-binding ligand (*L*) concentrations, from < 0.25 nM *L* in the very low chl surface waters west of STR, to > 0.5 nM *L* in the higher chl surface waters of the Ona Basin (Barbeau et al., 2006; Buck et al., 2007). While changes in Fe(III)-organic ligand concentration have been previously observed in conjunction with artificial Fe fertilizations, this is some of the first data indicating that ligand gradients can also be identified in regions of natural Fe fertilization. We observed decreases in *L* in near surface waters relative to deeper waters, indicative of a photochemical sink. Photo-reactive functional groups are seemingly prevalent in marine siderophores (Barbeau et al. 2003; Butler 2005), and under irradiated conditions, with a laboratory solar simulator, the ability of some of these siderophores to dissolve Fe from particles is enhanced (Borer et al. 2005). Further, recent work has shown that the biological uptake of iron from ambient ligands is significantly enhanced under natural sunlight (Maldonado et al., 2005).

## Phytoplankton

Accumulation of phytoplankton biomass in the ocean can be limited by various factors including grazing, sinking, advection, temperature, light and nutrients (Mitchell and Holm-Hansen, 1991). Our study region has weak gradients in temperature and surface light, but strong gradients in phytoplankton biomass, implying potential nutrient limitation. Understanding the connection between Fe limitation and carbon export in the Southern Ocean is essential for understanding global biogeochemical fluxes. Presently, there is more than a 3-fold uncertainty in estimates of organic carbon export flux (EF) of the Southern Ocean between global satellite estimates and an inverse model estimate (Schlitzer, 2002). When blooms exhaust available Fe, senescence may lead to accelerated rates of organic carbon export to the ocean interior. Diagnosis of the phytoplankton physiology is important to understand the relative stage of blooms with respect to available Fe.

### *Spatial and seasonal structure of phytoplankton*

The section across the ACC to the Shackleton Shelf shows that the core of the ACC water was warm, and had low values for Fe, Mn and chl-a during LMG0402 (Figure 4; Measures et al., 2006). Highest values of chl-a were in waters on the east side of the front that had relatively low Fe but high Mn, indicating these waters had a shelf source but Fe may have been drawn down by phytoplankton. During winter (NBP0606) phytoplankton abundance was about 6-7 times lower compared to summer (LMG0402). However, during winter offshore ACC waters had higher phytoplankton abundance than shelf and Bransfield Strait waters. In winter, shelf waters and Bransfield Strait water were much more deeply mixed than winter the ACC waters. Since iron was relatively high for all waters during winter, especially on the shelf and in Bransfield Strait, light limitation in these deep mixed layers is considered to be the cause of the low chl-a in shelf and Bransfield water. During winter, larger phytoplankton (diatoms and >10 μm autotrophic dinoflagellates) were very low, however Fe addition incubation during NBP0606 resulted in growth of diatoms indicating that seed populations of diatoms were present and able to grow well when provided sufficient light in the incubators.

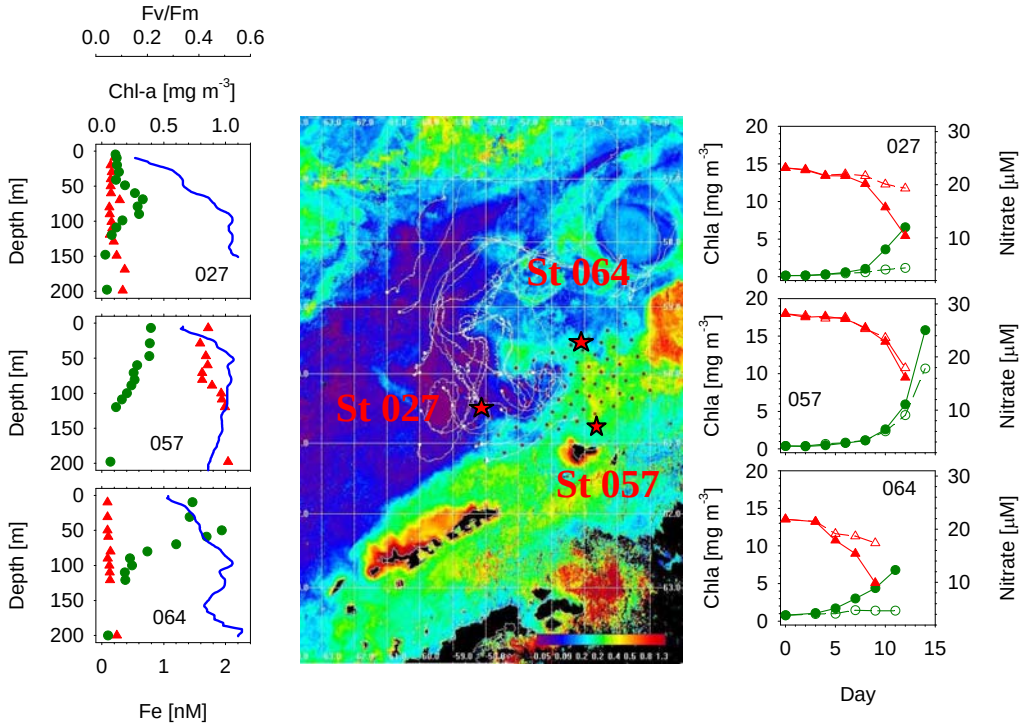


**Figure 7.** Locations of iron-enrichment experiments for representative stations are shown on a MODIS chl-a composite image for February (red stars). See Figure 5 for T-S characteristics for these stations. Left panels: the profiles of Fv/Fm, chl-a and Fe where red triangles (▲) represent Fe, green solid dots (●) represent chl-a and blue solid lines (–) represent Fv/Fm. Right panels: time-series of chl-a and nitrate in the growth experiments where green circles (○) represent chl-a of controls, green solid dots (●) a represent chl-a of Fe-amended treatments, red triangles (△) represent nitrate of controls, and red triangles (▲) represent nitrate of Fe-added treatments.

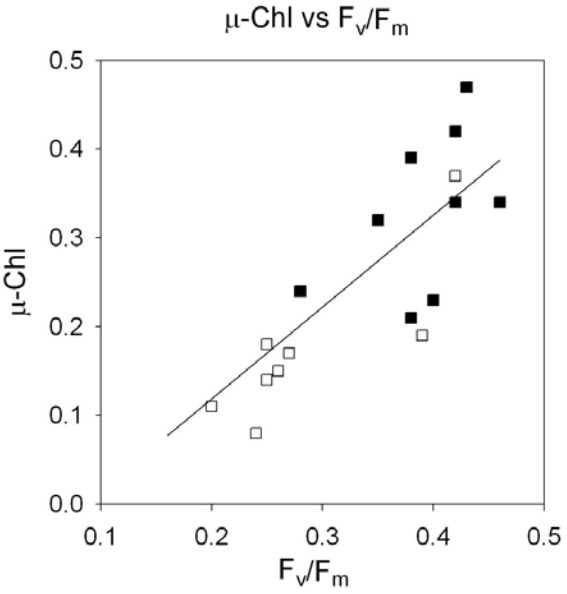


**Figure 8.** Relationship between phytoplankton growth rates based on changes of chl over time (µ-chl), and $F_v/F_m$ for incubation experiments. Open symbols are data from controls and filled symbols are for Fe amended treatments.

Figure 7 illustrates phytoplankton community spatial structure based on a satellite-derived chl-a map corresponding to LMG0402. Vertical profiles of several parameters are shown in Figure 7 for the representative stations where we collected mixed layer water for iron enrichment experiments. Chl-a was highest in mixed water over Ona Basin but iron was low in the euphotic zone at this station, suggesting that phytoplankton depleted the iron. Low chl-a and low iron were observed at station 27 in the core of the ACC intrusion west of the STR, with a typical deep chl-a maximum (Holm-Hansen and Hewes, 2004). Relatively low chl-a in high Fe shelf water (station 57) suggests that light and deep mixing may play roles in limiting phytoplankton biomass accumulation on the shelf (Mitchell and Holm-Hansen, 1991; Mitchell et al., 1991; Mitchell et al., 2006). Highest values for $F_v/F_m$ were observed near the base of the photic zone with a value approaching 0.6 at station 64. Values of $F_v/F_m$ in near-surface waters were low for these stations profiled in mid-day. Lowest values for $F_v/F_m$ (~0.2) were found in the mixed of station 27 where the ACC surface waters were low in Fe.

***Fe amendment Incubation Experiments***

During LMG0402 (summer) and NBP0606 (winter), incubation studies were used to diagnose the Fe limitation status of the phytoplankton community for different water types and the role of Fe in regulating plankton community structure (Mitchell et al., 2006; 2007; Hopkinson et al., 2007). The spatial distribution of chl-a from satellite images provided to the ship within 24 hours of satellite overpass, and the Fv/Fm data collected during profiles were used to specify archetypal stations used for Fe-amendment experiments.

Table 2 summarizes 3 of the 12 incubation experiments for water taken from mixed layers at stations with representative water types (Figure 5; Hopkinson et al., 2007). The station positions are shown in the satellite chl-a map (Figure 7). Experiments XB (blue ACC water), XS (shelf water), and XM (mixed water) were set up with mixed layer water from the stations shown in Figure 7. For experiments XB and XM, chlorophyll increased faster with iron amendment compared to controls. By the end of the experiment for XB and XM, chlorophyll values were 5-10 times greater than the controls with strong drawdown of nitrate and silicate in iron treatments. In iron treatments Si:N drawdown ratios were approximately 1 while the controls had SI:N drawdown ratios of approximately 2, consistent with heavier diatom silicification under iron stress as reported previously (Takeda 1998; Hutchins and Bruland 1998). For experiment XS, chl-a growth was substantial in both Fe amended and control bottles with no significant difference between these treatments. Relative to the initial values, $F_v/F_m$ increased in iron treatments for XB from 0.2 to 0.4 and XM from 0.27 to 0.35. For experiment XS, $F_v/F_m$ was relatively high (0.45) from the outset and did not change in iron treatments or controls. Figure 8 indicates that the growth rate for the phytoplankton in the experiments was well correlated to $F_v/F_m$. In our analyses of incubation experiment results from LMG0402 and NBP0606, we are exploring the following questions: 1) what is the maximum carrying capacity of the system for phytoplankton biomass? 2) What is the relative Fe:C:N:Si drawdown ratio, and how do these ratios change under high and low light conditions and with different communities? 3) Are phytoplankton on the shelf light-limited? 4) What is the relative importance of Fe vs. light limitation for phytoplankton in the deep chlorophyll maximum west of the STR? Our incubation experiment results from LMG0402 have been published in Hopkinson et al. (2007).

**Table 2.** Summary of results for controlled iron amendment growth experiments accomplished during LMG0402 for the stations shown in Figure 7. The stations were characterized as low iron ACC water (27), high iron shelf water (57) and low iron mixed water (64). The experiments for blue ACC water, Shelf water and Mixed water are referred to as XB, XS and XM, respectively. See Figure 7 for hydrographic profiles of the stations and for the chl-a and $NO_3$ time-series graphs for these incubation experiments and Figure 5 for T-S relationships for these stations. Data published in Hopkinson et al. 2007.

| Station | Water | Expt | Treatment | Chl a [mg $m^{-3}$] | | $F_v/F_m$ [rel] | | μ | $NO_3$:Chl | $SiO_3$:Chl | $SiO_3$:$NO_3$ |
|---|---|---|---|---|---|---|---|---|---|---|---|
| No. | Type | ID | Type | $T_{initial}$ | $T_{final}$ | $T_{initial}$ | *Max* | [$d^{-1}$] | [g:g] | [g:g] | [M:M] |
| | | | | | | | | | | | |
| 27 | ACC | XB | Control | 0.15 | 0.85 | 0.23 | 0.31 | 0.14 | 214 | 557 | 2.10 |
| | | | +Fe | | 6.35 | | 0.38 | 0.39 | 119 | 143 | 0.98 |
| | | | | | | | | | | | |
| 57 | Shelf | XS | Control | 0.44 | 11.82 | 0.43 | 0.43 | 0.31 | 117 | 128 | 0.86 |
| | | | +Fe | | 15.66 | | 0.43 | 0.34 | 110 | 109 | 0.80 |
| | | | | | | | | | | | |
| 64 | Mixed | XM | Control | 0.87 | 1.74 | 0.35 | 0.35 | 0.05 | 279 | 814 | 1.87 |
| | | | +Fe | | 8.10 | | 0.40 | 0.23 | 157 | 201 | 1.00 |

*Phytoplankton biomass and hydrographic structure*

To better understand the distributions in the phytoplankton community hydrographic, nutrient and element (iron, manganese, and aluminum) concentration data collected in austral summer 2004 during the LMG0402 and AMLR 2004 2-ship survey were used to examine the influence of upwelling and horizontal mixing to phytoplankton biomass in the region of Elephant Island and South Shetland Islands, Antarctica (Table 3; Hewes et al. 2007). Temperature/Salinity property analysis and changes in trace metal and nutrient concentrations show that horizontal mixing of shelf waters, not upwelling from depth, is correlated with the phytoplankton biomass of phytoplankton in the upper mixed layer (UML). The interaction between changing UML depth and nutrient and element concentrations in the UML results in a unimodal distribution of phytoplankton biomass centered at intermediate salinities of ~34. Principal Component (PC) analysis of hydrographic and chemical observations resolved three components that accounted for 99 % of the variability in nutrient and element concentrations. The first PC accounted for a conservative loss of nutrients through dilution across a latitudinal salinity gradient. The second and third PCs separated mixed layer depth and nutrient consumption. Although these two PCs accounted for just 20 % of the variability in the data matrix, they accounted for 65 % of the variability in mean phytoplankton biomass, and recreated the unimodal distribution of chlorophyll concentration when modeled across a salinity gradient. These findings of Hewes et al. (2007) indicate that the distribution of phytoplankton biomass is structured by the horizontal mixing of nutrient rich shelf waters that supply iron, and also result in shoaling of the UML, in the vicinity of our main field survey domain. These analyses have been supported by independent analysis of hydrographic data and short-lived radium tracer studies carried out by our WHOI collaborators on AMLR 2006 and NBP0606 (Dulaiova et al., 2007).

**Table 3.** Average biological, chemical and physical characteristics of the water columns for 4 water zones classified in the South Shetland Islands and Elephant Island region as related to isopycnal surfaces of 27.6 and 27.4 Kg $m^{-3}$. Number of stations and average depth to ocean bottom (meters) is given for each water zone. Average temperature, salinity and oxygen from CTD data binned at 1 m intervals, and silicate, silicate:nitrate ratio, Al, Fe, and Mn from discrete water bottle samples (number of silicate and trace metal samples given). These data for isopycnal surfaces were obtained at depths at which density was $\sigma_t = 27.6 \pm 0.05$ and $\sigma_t = 27.4 \pm 0.02$ Kg $m^{-3}$. From Hewes et al. (2007)

| | "ACC-Like" | | | | | |
|---|---|---|---|---|---|---|
| Water Zone | 1A | | 1B | | 2A | |
| Isopycnal | 27.6 | 27.4 | 27.6 | 27.4 | 27.6 | 27.4 |
| No. of Stations | 49 | | 31 | | 25 | |
| Depth | 362 ± 96 | 147 ± 32 | 237 ± 55 | 104 ± 18 | 192 ± 42 | 84 ± 20 |
| Temp,°C | 2.0 ± 0.3 | 0.9 ± 0.7 | 1.7 ± 0.3 | 0.1 ± 0.5 | 1.5 ± 0.4 | 0.3 ± 0.3 |
| Salinity | 34.54 ± 0.05 | 34.20 ± 0.07 | 34.51 ± 0.05 | 34.14 ± 0.06 | 34.50 ± 0.06 | 34.15 ± 0.04 |
| $O_2$, ml $l^{-1}$ | 4.1 ± 0.2 | 5.9 ± 0.5 | 4.3 ± 0.3 | 6.5 ± 0.4 | 4.5 ± 0.5 | 6.6 ± 0.5 |
| No. of Nut | 7 | 22 | 2 | 15 | 11 | 32 |
| SiOH, µM | 78 ± 1 | 50 ± 6 | 72 ± 1 | 55 ± 6 | 74 ± 3 | 58 ± 6 |
| SiOH:NO3 | 2.2 ± 0.0 | 1.5 ± 0.1 | 2.1 ± 0.1 | 1.8 ± 0.2 | 2.1 ± 0.1 | 1.9 ± 0.2 |
| No. of TM | 4 | 14 | 3 | 11 | 3 | 17 |
| Al, nM | 1.3 ± 0.1 | 1.2 ± 0.3 | 1.1 ± 0.3 | 1.1 ± 0.1 | 1.0 ± 0.1 | 1.1 ± 0.1 |
| Fe, nM | 0.66 ± 0.19 | 0.35 ± 0.16 | 0.47 ± 0.08 | 0.35 ± 0.16 | 0.65 ± 0.25 | 0.58 ± 0.41 |
| Mn, nM | 0.21 ± 0.09 | 0.17 ± 0.07 | 0.39 ± 0.18 | 0.87 ± 0.66 | 0.42 ± 0.28 | 1.12 ± 0.66 |

| | "Weddell-Like" | | | | | |
|---|---|---|---|---|---|---|
| Water Zone | 2B | | 3 | | 4 | |
| Isopycnal | 27.6 | 27.4 | 27.6 | 27.4 | 27.6 | 27.4 |
| No. of Stations | 22 | | 29 | | 35 | |
| Depth | 203 ± 37 | 82 ± 24 | 224 ± 56 | 61 ± 32 | 195 ± 71 | 61 ± 41 |
| Temp,°C | 0.5 ± 0.4 | 0.5 ± 0.3 | 0.1 ± 0.2 | 0.7 ± 0.3 | -0.1 ± 0.5 | 0.6 ± 0.2 |
| Salinity | 34.42 ± 0.05 | 34.16 ± 0.03 | 34.38 ± 0.04 | 34.18 ± 0.03 | 34.38 ± 0.04 | 34.17 ± 0.02 |
| $O_2$, ml $l^{-1}$ | 5.6 ± 0.5 | 6.9 ± 0.3 | 6.1 ± 0.3 | 7.1 ± 0.2 | 6.3 ± 0.6 | 7.1 ± 0.3 |
| No. of Nut | 9 | 28 | 6 | 33 | 11 | 21 |
| SiOH, µM | 78 ± 2 | 67 ± 4 | 81 ± 2 | 72 ± 2 | 78 ± 2 | 72 ± 1 |
| SiOH:NO3 | 2.4 ± 0.1 | 2.3 ± 0.2 | 2.6 ± 0.1 | 2.5 ± 0.1 | 2.5 ± 0.0 | 2.5 ± 0.0 |
| No. of TM | 4 | 15 | 4 | 13 | 7 | 13 |
| Al, nM | 1.4 ± 0.0 | 1.6 ± 0.2 | 1.9 ± 0.3 | 2.0 ± 0.4 | 1.6 ± 0.2 | 2.0 ± 0.7 |
| Fe, nM | 1.18 ± 0.77 | 1.15 ± 0.53 | 1.97 ± 0.06 | 1.86 ± 0.31 | 2.85 ± 0.41 | 3.05 ± 1.50 |
| Mn, nM | 1.48 ± 1.03 | 2.78 ± 1.32 | 2.15 ± 0.34 | 2.47 ± 0.23 | 1.64 ± 0.14 | 4.23 ± 3.25 |

Photosynthetic physiology

Phytoplankton acclimation to light, temperature or nutrient limitation causes changes in cellular pigment concentrations, ratios of photoprotective to photosynthetic pigments, chl-a specific spectral absorption ($a^*_{ph,}$), and maximum quantum yield of photosynthesis ($\Phi_{max}$) (Falkowski et al., 1985; Dubinsky et al., 1986; Mitchell and Kiefer, 1988; Challup and Laws, 1990; Sosik and Mitchell, 1991; 1994; Geider et al., 1998; Moisan and Mitchell, 1999). We expect that severely Fe stressed communities will have low $\Phi_{max}$ attributable in part to high ratios of photoprotective relative to photosynthetic pigments and in part to stress-related inefficiencies of the photosynthetic electron transport system. *In vivo* chl-a fluorescence induction and decay allows relative estimates of an initial ($F_o$) and maximal fluorescence yield ($F_m$). The variable fluorescence ($F_v=F_m-F_o$) can be related to the fraction of functional reaction centers (Greene et al., 1994; Kolber et al., 1994); $F_v/F_m$ is often used as a convenient index of iron-limitation (Behrenfeld et al., 1996; Boyd et al., 2000; Olson et al., 2000). Since nutrient stress can change ratios of photoprotective to photosynthetic pigments, chl-a specific absorption and $\Phi_m$, these measurements were made to interpret changes in photosynthetic physiology caused by Fe limitation. Fast Repetition Rate fluorometry (FRRF) profiles during the survey stations provided spatial and vertical distribution of the physiological status of phytoplankton (Figure 7). Various parameters derived from the variable fluorescence data are well correlated with iron limitation (Hopkinson et al., 2007). The $F_v/F_m$ values for incubations provide an excellent index of the phytoplankton growth rate (Figure 8). These results were fundamental to our interpretation of iron enrichment incubation studies published in Hopkinson et al. (2007).

Photosynthesis vs Irradiance (PvsE) experiments were done at various depths for representative stations throughout our survey grid. PvsE curves in Figure 9 indicate that values for $P^B_{max}$ (maximum rate of carbon fixation per chlorophyll) were lowest for iron poor, low chlorophyll ACC waters to the west of STR (Mitchell et al. 2006). Shelf waters exhibited intermediate values for $P^B_{max}$, while mixed waters in the frontal gradients had highest values. We also made detailed measurements of phytoplankton spectral absorption coefficients. Spectral absorption and PvsE data were used to compute $\phi_{max}$, the maximum quantum yield of photosynthesis in the light limited part of the PvsE curve. In Figure 10 values of $P^B_{max}$ and $\phi_{max}$ for the surface mixed layer are overlaid on the February satellite map of surface chlorophyll. The data indicate strong spatial gradients in both of these parameters. Values for the iron poor low chlorophyll waters were consistently lower than for the shelf or mixed water. Highest values were found in the mixing zones between ACC and shelf waters. This variability needs to be better understood in order to develop accurate models of ocean primary production to be used with ocean color satellite data. Figure 11A provides a comparison of the vertical structure of salinity, temperature and chlorophyll in the upper 500 m of ACC water west of STR during LMG0402 (summer) and NBP0606 (winter). For off shore waters of the ACC, chl-a in the upper 100 m was similar to, or higher, during winter as compared to summer. Figure 11B is a comparison of PvsE curves for typical ACC water west of STR during summer and winter. The chl-a normalized primary production has a higher $P^B_{max}$ in winter, and the initial slope ($\alpha$) and the maximum quantum yield computed from the $\alpha$ and phytoplankton absorption are also both higher during winter compared to summer. These results are surprising discoveries that indicate global primary production of the ACC during winter may be higher than previously reported.

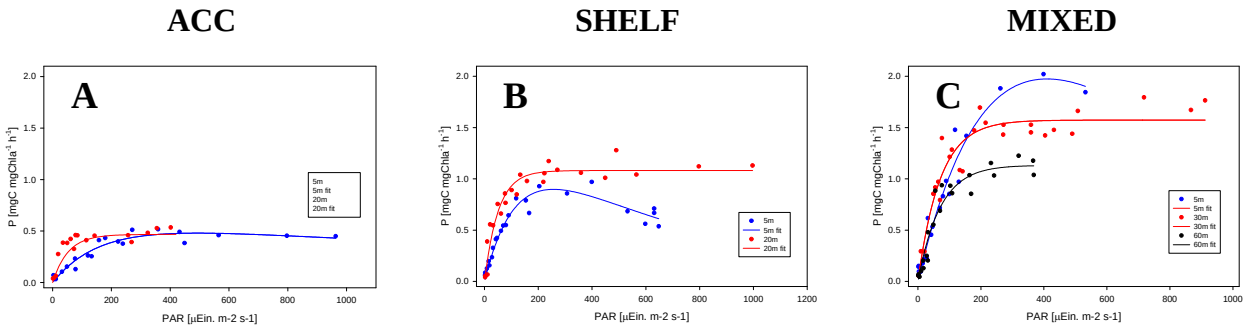


**Figure 9.** Photosynthesis vs Irradiance curves (PvsE) for phytoplankton sampled in different water masses. **A.** Low chlorophyll ACC water, **B**. Shelf water, **C.** Mixed waters in the frontal gradient.

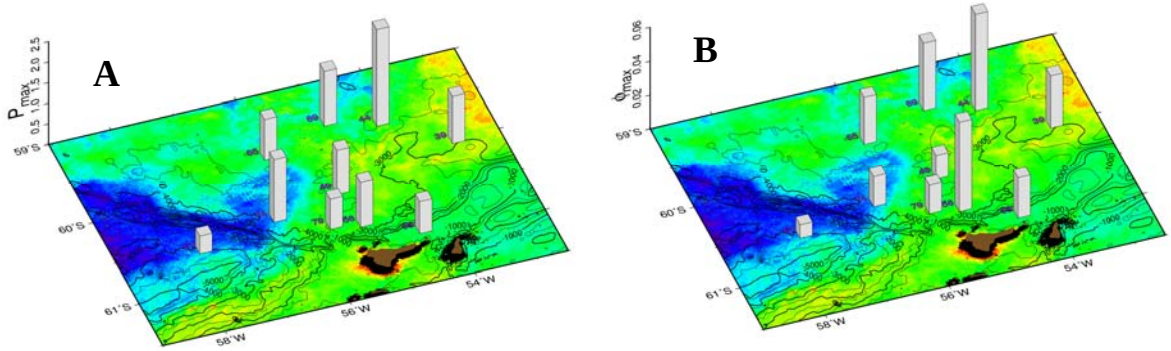


**Figure 10.** Summary of spatial distribution of photosynthetic physiology. **A**. Maximum rate of chlorophyll-specific carbon fixation $P_{Bmax}$, and **B.** the maximum quantum yield of photosynthesis $\phi_{max}$. Values of $P_{Bmax}$ $\phi_{max}$ were highest in shelf waters or mixed waters along the frontal gradient between ACC and Shelf waters.

*Modeling Photosynthesis*

In collaboration with other Southern Ocean projects, we have used the methods pioneered in our lab (Sosik and Mitchell, 1992; Moisan and Mitchell, 1999) to compute quantum yields for JGOFS and SOFEX data (Hiscock et al., 2006; 2007). Hiscock et al. (2007) have concluded that iron fertilization in the Southern Ocean has a larger effect on the light-limited $\phi_{max}$ than on $P^B_{max}$. Hence, much of the increase in primary production, and associated export flux, related to iron fertilization may be a consequence of elevated rates of primary production for the light limited part of the water column. Combining our results summarized in Figures 9 and 10 with findings from our collaboration with other projects, we are developing new models for Southern Ocean NPP and EF. Combining our historic data, we have leveraged the results and findings regarding NPP and EF for a new NASA-funded synthesis of data collected under this award, and data collected on previous projects. This NASA synthesis to improve satellite models for estimating POC export flux is part of the Southern Ocean GasEX program and our work under this NSF award in collaboration with our WHOI colleagues resulted in key findings on photosynthesis and the relationships between NPP and EF that were used in our NASA proposal.

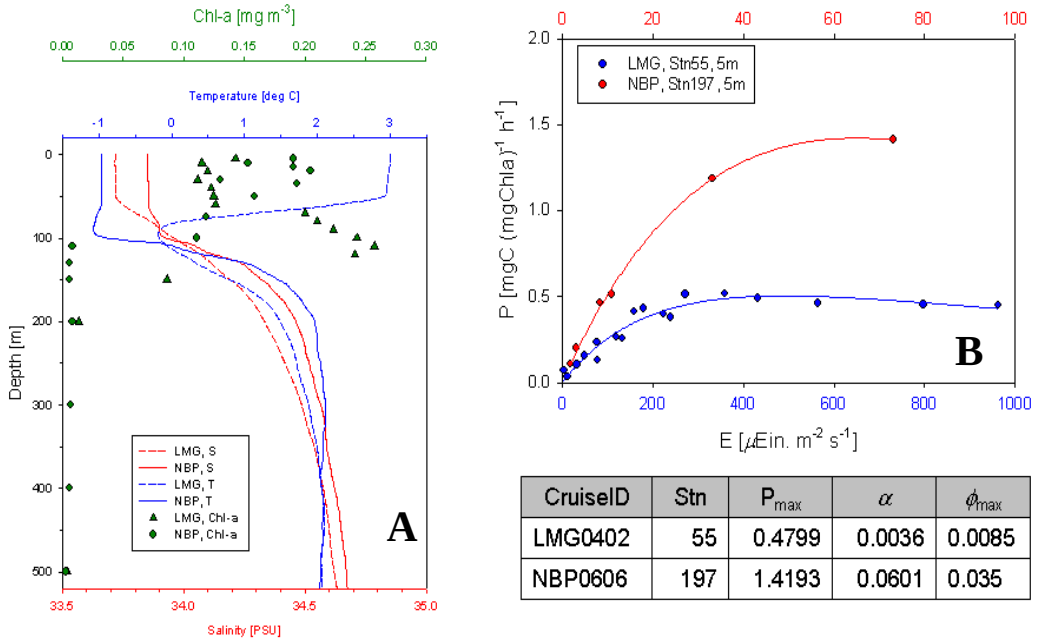


| CruiseID | Stn | $P_{max}$ | $\alpha$ | $\phi_{max}$ |
|---|---|---|---|---|
| LMG0402 | 55 | 0.4799 | 0.0036 | 0.0085 |
| NBP0606 | 197 | 1.4193 | 0.0601 | 0.035 |

**Figure 11 A**. Profiles of temperature, salinity and extracted chl-a for typical ACC station during summer (LMG) and winter (NBP). **B.** Photosynthesis vs irradiance (PvsE) relationship for mixed layer sample from stations shown in **A**. Table summarizes the PvsE fitted parameters and $\Phi_{max}$ for curves shown in **B**. Surprisingly high chlorophyll and rates of photosynthesis were observed in ACC waters during winter.

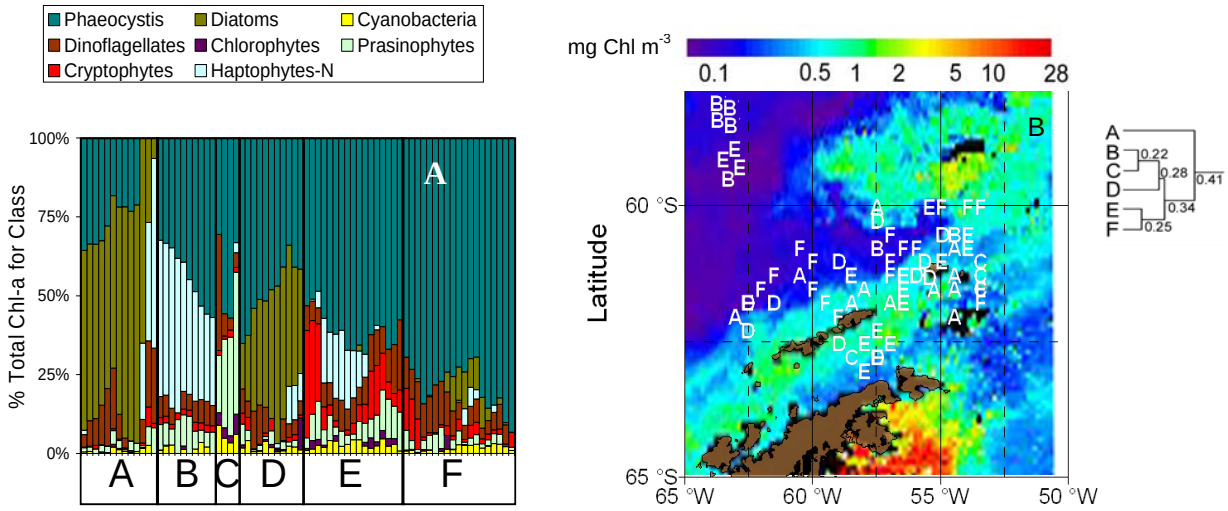


**Figure 12**. **A)** Objective estimate of phytoplankton community taxonomic structure for stations sampled during AMLR2004 and LMG0402. Cluster analysis was performed upon CHEMTAX derived relative algal class abundance that utilized HPLC pigment assay to define six different phytoplankton communities. **B)** Chlorophyll map from SeaWiFS for February 2004 has phytoplankton communities clusters A-F overlaid at their respective station position.

Figure 12 illustrates phytoplankton community clusters based on CHEMTAX analysis (Mackey et al., 1996; Wright et al. 1996) of HPLC pigments for summer (Mitchell et al., 2006). ACC waters were dominated by nanoplankton (cells 2-20 μm group B), the Bransfield Strait was dominated by cryptophytes and flagellates (group E) or dominated by microplankton (cells >20 μm) diatoms (A and D), and the shelf regions of the Shelter Islands and Elephant Island were dominated by microplankton diatoms (A and D) or cryptophytes and flagellates (group E). The low chlorophyll containing waters of the ACC (upper left portion of Figure 5B) were dominated by groups B and E (this group contains a significant portion of cryptophyte-like pigments). These pigment-based clusters can be related to low Fe ACC, high Fe Shelf or mixed waters. Flow cytometry, HPLC pigment analysis, and classic microscopy have been used to characterize phytoplankton communities (Selph et al., 2006). In our synthesis efforts community structure including size distributions and taxonomic affiliation will be used to understand how variations of the community structure and photosynthetic acclimation regulate primary production.

The chl-a normalized spectral absorption of particles ($a_p$), phytoplankton ($a_{ph}$), and detritus ($a_d$) are shown for summer (LMG0402) and winter (NBP0606) in Figure 13. Relatively more detrital absorption during winter will affect bio-optical algorithms for chl-a retrieval. Also, the higher detrital absorption during winter offers evidence that heterotrophic processes are enhanced in winter relative to autotrophic processes. Our detailed studies of ocean spectral reflectance (ocean color) and the inherent optical properties (absorption, beam attenuation, and backscattering) for LMG0402, AMLR2004, AMLR2006 and NBP0606 are being used to evaluate bio-optical models for winter and summer and to improve satellite algorithms for retrieval of chl-a and primary production.

**Estimates of POC Export**

During the AMLR2006 summer cruise $^{234}$Th-derived POC export was ~10-x higher in waters north of the shelf break east of the Shackleton Gap compared to open ocean stations west of the Shackleton Transverse Ridge (See Charette findings ANT 04-43869). We have assembled a global Southern Ocean data set of POC export flux (EF) and net primary production (NPP) including data from AMLR2006 and NBP0606. As found by others, there is relatively large variance in the ratio EF/NPP leading to significant uncertainty in estimates of EF using satellite data and models (Figure 1B). To constrain global carbon cycle models applied to satellite data, this variance must be better understood. Our $^{234}$Th-derived POC flux data from AMLR 2006 indicate that natural Fe fertilization may generate higher export flux than estimates made for *in situ* Fe addition experiments, in part perhaps because the experiments were not able to observe the end of bloom dynamics after Fe exhaustion. When blooms exhaust available Fe, senescence may lead to accelerated rates of organic carbon export to the ocean interior. Thus diagnosis of the phytoplankton physiology is important to understand the relative stage of blooms with respect to available Fe. Variability in EF:NPP for our cruises will be interpreted with respect to the naturally occurring communities that we find to be differentiated in water types that have different rates of Fe supply and this understanding will be used in improved models applied to satellite data as part of our NASA-funded project.

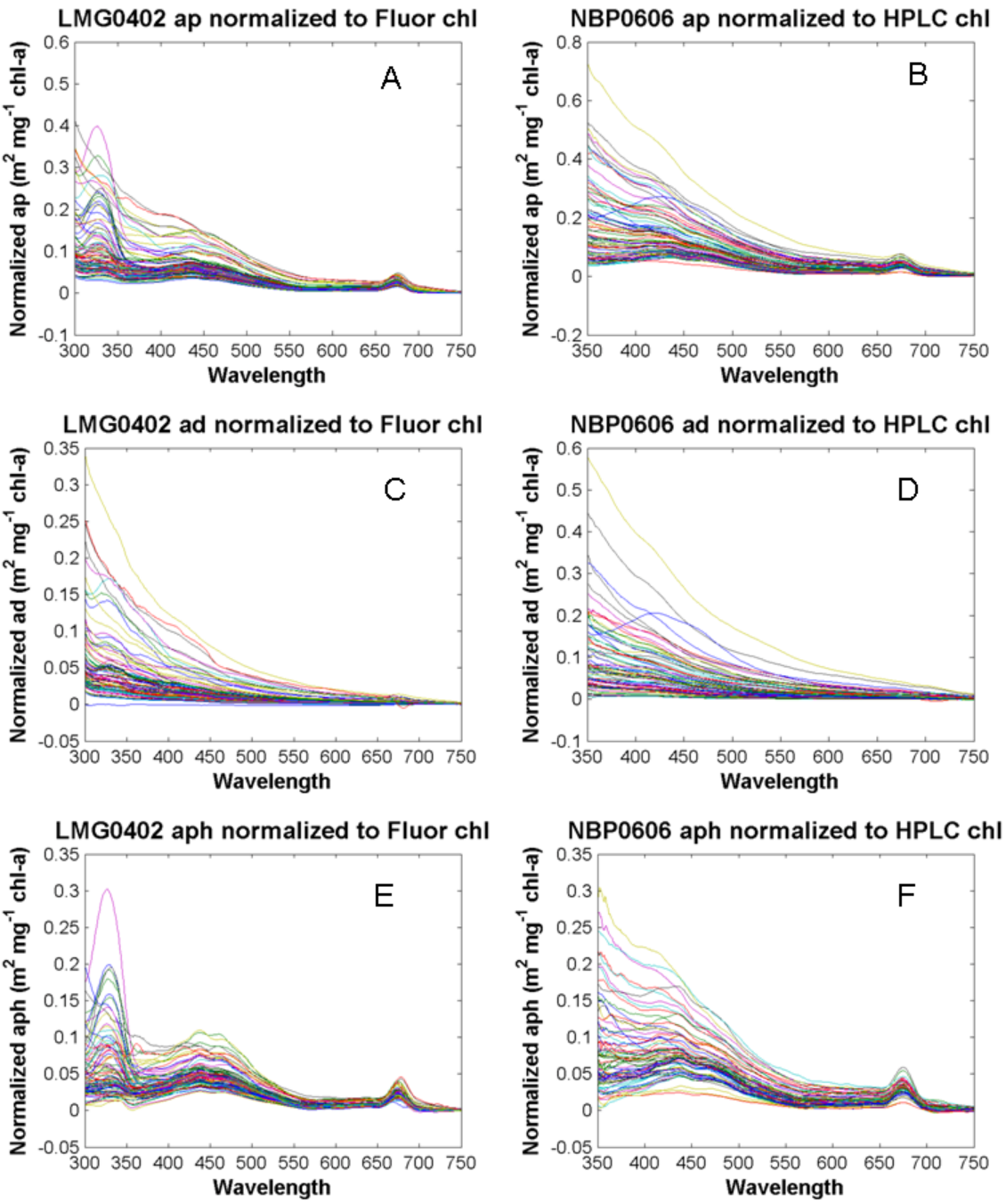


**Figure 13.** Absorption spectra normalized to chl-a for total particulates (ap), detrital particulates (ad) and phytoplankton (aph) for summer (LMG0402, left panels) and winter (NBP0606, right panels. Relatively more detrital absorption was observed during winter, an indication that heterotrophic processes during winter degrade phytoplankton pigments causing detrital material to accumulate.

**Microbial Communities and Dynamics**

While the supply of Fe may set the proximate limit for accumulation of phytoplankton biomass, the coupling between the microbial phototrophic and heterotrophic cells is fundamental to understanding the cycling of Fe within the plankton community and may have implications for bloom longevity. Since smaller cells have a greater surface area:volume ratio, nanoplankton and bacteria could have an advantage over large cells for uptake of limited resources. Church et al. (2000) reported that organic carbon was more effective than Fe in stimulating bacterial growth in the Ross Sea, indicating DOC limitation. These results are consistent with reports from the California upwelling regime where it has been hypothesized that bacterial production may be limited primarily by organic matter (even in Fe-poor regions) and Fe-limitation may occur rapidly after carbon-limitation is relieved (Hutchins et al., 1998; Kirchman et al., 2000; Bruland et al., 2001).

The goals of microbial studies during LMG0402 and NBP0606 were to quantify Fe and C fluxes into bacteria and phytoplankton and to elucidate the significance of the microbial loop in mediating and regulating these fluxes along the strong chl-a gradients near STR. Large differences between the ACC and mixed water were found for bacteria-mediated fluxes of carbon (as well as coupled Fe fluxes, assuming constant bacterial Fe:C). During the 2004 summer cruise, large differences between the ACC and mixed water were found for bacteria–mediated fluxes of carbon and coupled Fe fluxes assuming constant bacterial Fe:C. Bacterial carbon demand (BCD), assuming bacteria growth efficiency to be 20%, for samples within the upper 30 m was 3 times higher in the mixed water (~54.15 mmol C $m^{-2}$ $d^{-1}$ at chl–a of 0.87 mg $m^{-3}$) than the ACC water (~17.67 mmol C $m^{-2}$ $d^{-1}$ at chl–a of 0.13 mg $m^{-3}$). Bacterial standing stocks in both zones were low (0.8 to $3x10^{11}$ $m^{-3}$). Bacterial carbon production (BCP) for samples within the upper 30 m was 3 times higher in the mixed water (~10.83 mmol C $m^{-2}$ $d^{-1}$) than that of the ACC water (3.53 mmol C $m^{-2}$ $d^{-1}$) The differences in BCP may be attributed to large differences in bacterial specific growth rates approximately 0.13 $d^{-1}$ and 0.34 $d^{-1}$ in the ACC and mixed water regions, respectively. The bacterial population growth rates were possibly controlled by protistan grazing and phage induced lysis. Strong grazing pressure would suggest a tight trophic coupling with higher trophic levels while phage-induced lysis would increase system respiration (Fuhrman, 1999). These results for LMG0402 demonstrate that bacterial population growth rates were moderate (ACC) to high (mixed), yet there was a strong control on population abundance, possibly by protistan grazing and phage induced lysis. Strong grazing pressure would suggest a tight trophic coupling with higher trophic levels while phage-induced lysis would increase system respiration (Fuhrman, 1999). Differences in the concentration of utilizable DOC between different water types were determined on the basis of bacterial yield and DOC decline in 0.6 μm filtrates. These incubations explored whether protistan grazing pressure maintains the observed low bacterial abundances, i.e., whether release from grazing will cause large population increases in 0.6 μm filtrates. Shifts in bacteria and archaea species composition across the survey region are being explored using 16S rRNA sequences from environmental DNA extracts.

The $^{234}$Th-based POC flux data from our 2006 AMLR cruise suggests that between 50-100m depth there is a significant decrease in export flux, equivalent to ~ 60 m mol C $m^{-2}d^{-1}$ or ~12 μg C $L^{-1}$ $d^{-1}$. Based on our 2004 measurements of bacterial carbon demand (0.07-6 μg C $L^{-1}$ $d^{-1}$), up

to half of this remineralization loss can be explained by bacterial utilization and solubilization processes. Protistan grazing of particle-associated bacteria can account for an additional component of this loss, and for the return of $^{234}$Th to the dissolved phase (Lee et al. 1993, Barbeau et al. 2001). These processes appear to be crucial in determining carbon export flux in our study region. Using our integrated data set of community structure, size of phytoplankton, NPP, EF and photosynthetic physiology, we are exploring methods to improve our ability to predict EF for satellite applications.

Results from the 2006 austral winter cruise (NBP0606) showed that BCP for samples within the upper 100 m was 2.80 mmol C $m^{-2}$ $d^{-1}$ in the ACC water and 1.30 mmol C $m^{-2}$ $d^{-1}$ in the mixed water, contrasting results with respect of summer 2004, still a significant BCP. Bacteria during winter (NBP0606) ranged between 0.8 to 3x$10^{11}$$m^{-3}$ overlapping the summer 2004 range. During the winter NBP0606 cruise, negligible bacterial carbon production and very low growth rates were observed for the ACC water in winter, but rates were measurable in the shelf and in the mixed zone. The bulk bacterial production is low, but there is always a fast growing fraction (the attached fraction). The rapidly growing fraction varies as a fraction of total bacteria varies across the study domain and the species that comprise the community also vary significantly (Malfatti et al., 2005). There is significant seasonal variation in community composition between our summer (LMG0402) and winter (NBP0606) cruises.

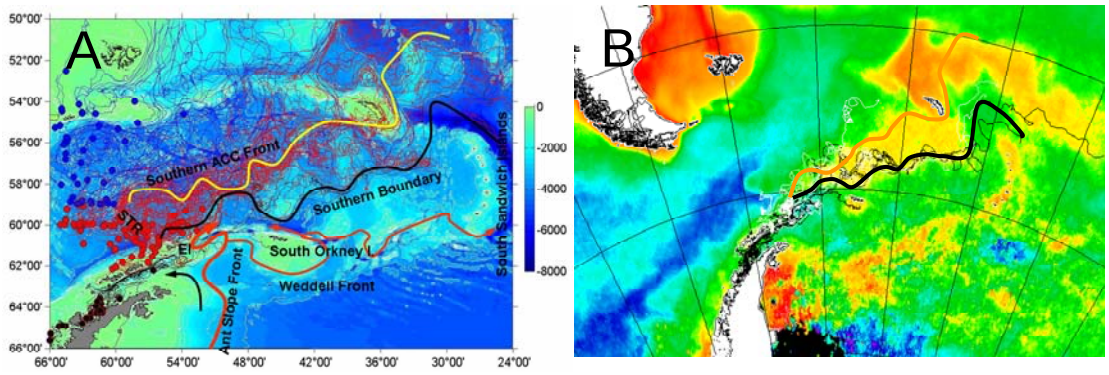


**Figure 14. A)** Drifter trajectories in the Southern Drake Passage. Black, red and blue dots and thin lines are deployment locations and trajectories of drifters deployed during RACER, AMLR and LMG0402. Thick yellow and black lines represent the SACCF and ACCSB, respectively, based on drifters released at the SACCF and modeling results (Schodlok et al., 2002). The red thick lines represent the Antarctic Slope and Weddell Fronts (Heywood et al., 2004). **B)** 10-year composite for SeaWiFS chla for October-March (1997-2006). Note that the high chl-a in the Southern Scotia Sea originates north of Elephant Island. We have discovered a strong jet of the SACCF that is steered by the Shackleton Transverse Ridge onto the shelf where it entrains high Fe shelf water that is mixed with ACC water and transported off-shelf.

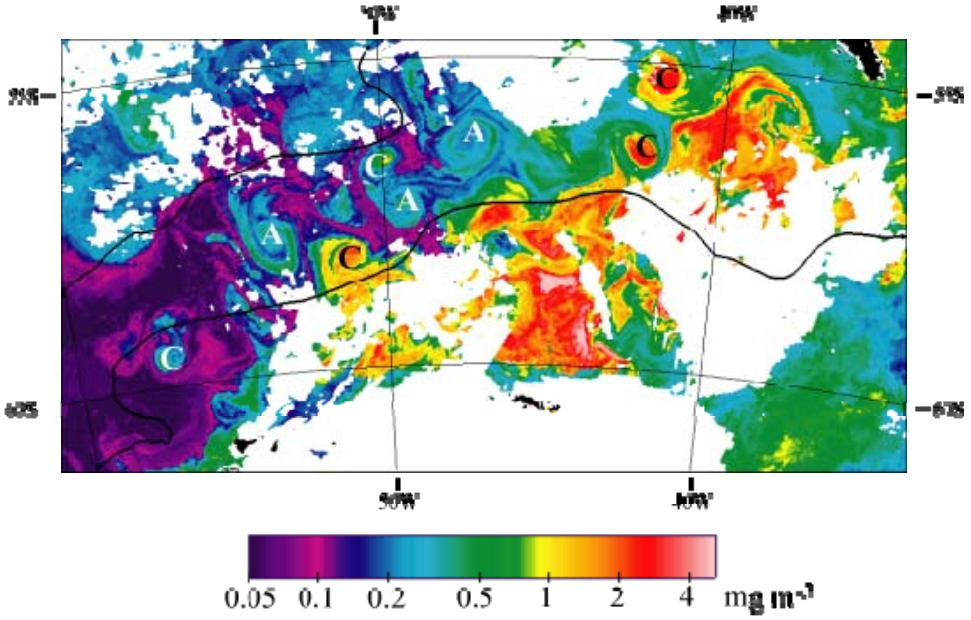


**Figure 15.** Image of chl-a distribution in the Southern Scotia Sea showing a string of cyclonic (C) and anticyclonic (A) eddies in the SACCF zone on Jan 26-30, 2005. The climatological mean positions of the PF (northern black curve) and SACCF (southern black curve) are shown (Fronts from Orsi et al., 1995). Right panels: Relationships between cyclonic eddy activity (RMS of the negative sea-level anomaly. **A,** Annual time series of Chl-a anomaly in October and RMS of negative SLA in September. **B**, Scatter plot between Chl-a anomaly in October and RMS of negative SLA in September. We have discovered strong correlation between eddy activity in the Southern Scotia Sea and the magnitude of phytoplankton chl-a downstream (Kahru et al. 2007). Further ship studies during September – October in the region would be required to better understand the mechanisms related to eddy activity and phytoplankton processes as regulated by light and iron.

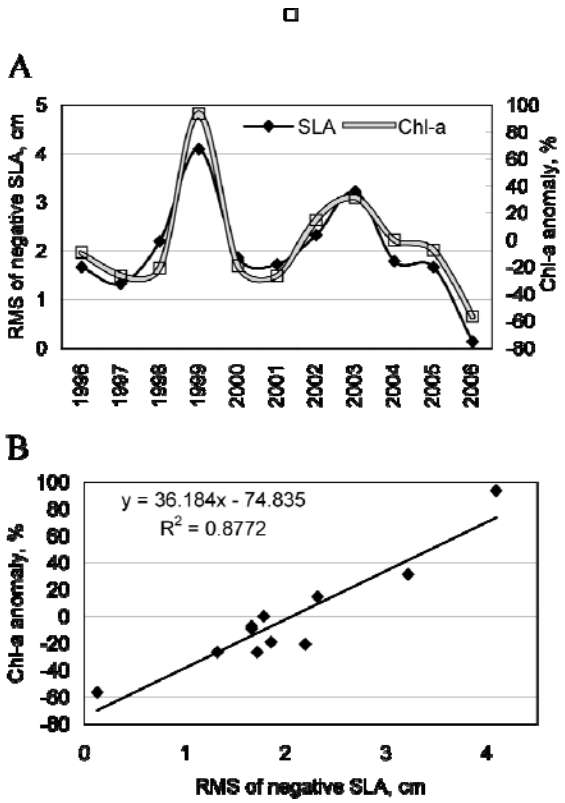

**Satellite time-series analysis**

The flow of the water that interacts with STR is bounded by the ACC Polar Front (ACCPF) to the north and the ACC Southern Boundary (ACCSB) to the south. Between these bounding fronts the SACCF can have large excursions, including the southward steering by the STR onto the Elephant Island shelf. The water that flows into the Southern Scotia Sea from STR is routinely supports some of the highest phytoplankton chl-a in the open Southern Ocean (Figures 1B, 6, and 14B). We believe that the entire Southern Scotia Sea is influenced by shelf-derived Fe that is delivered by the strong off-shelf transport mechanisms described above and in reports by our collaborators. The seasonal and interannual variability of the ACC may influence the southerly flow of the SACCF along the STR toward the shelf and the strength of the jet through the Shackleton Gap, and may in turn influence the off-shelf transport strength of the iron-enriched shelf water. By studying the satellite-derived time-series of SST and sea surface elevation fronts we are exploring this hypothesis. Analysis of the drifter trajectories indicate that ACC water steered by STR through Shackleton Gap is coherent through the entire Southern Scotia Sea. Altimetry and drifter analyses have revealed significant eddy activity along the ACCSB with implications for phytoplankton productivity (Figure 15, Kahru et al. 2007). Statistical analysis of the sea level anomaly derived from time-series of satellite altimetry, and chl-a anomaly derived from time-series of ocean color data indicate significant interannual variability in eddy activity and chl-a and correlations between the two with a 1-month time-lag (Figure 15, Kahru et al., 2007). The high biomass in the southeast region of the Scotia Sea suggests that there may be significant iron transported off the shelves of South Orkney, South Sandwich and South Georgia Islands. Verification of this hypothesis required future ship surveys with detailed hydrographic and trace metal analysis as we have carried out near Elephant Island and STR.

**Summary of Findings**

We executed a complex interdisciplinary research cruise near the Shackleton Fracture Zone on the R/V LM Gould during February - March, 2004 and on R/V NB Palmer July – August, 2006. The NSF-sponsored cruises were also complemented by NOAA AMLR summer cruises in 2004 and 2006. During LMG0402 and NBP0606 we carried out operations 24 hours a day and occupied approximately 100 stations each cruise (see activities report for details on NBP0606). We demonstrated that complex physical mixing processes can transport iron in shelf waters to the open ACC where phytoplankton blooms occur. Strong gradients in horizontal mixing of the major water masses were associated with gradients in iron distribution, plankton biomass, and plankton rate processes. This work will prove important for understanding iron regulation of plankton communities in the Southern Ocean and will be relevant for modeling the response to climate change of the Southern Ocean carbon cycle.

Ship and drifter data confirmed intense mesoscale eddy activities enhance horizontal mixing in the Ona Basin and on the shelf north of Elephant Island. Satellite analysis of fronts and eddies using altimetry documented strong correlations between eddy activity along the ACCSB and blooms of phytoplankton throughout the Southern Scotia Sea. Both in summer and winter, mixing between the ACC and shelf waters is associated with mesoscale eddy activities as it is transported offshore from the Elephant Island Shelf. North of the shelf break, values of eddy kinetic energy (EKE) field computed from the drifter data were very high for the main branches

of the SACCF along STR and also eastward along the shelf break. These two branches re-join to the east of Ona Basin. These EKE maxima along the main flow path of the SACCF imply strong horizontal eddy mixing of the iron-rich shelf waters and the iron-poor ACC waters. During NBP0606, extremely high values of trace metals, including iron, were found by the University of Hawaii group led by Christopher Measures (ANT 04-43403). High values were found in deep mixed layers up to 200 m deep on the shelf. During LMG0402, summer values were lower in the stratified surface waters suggesting that the phytoplankton remove significant fractions of the shelf-derived iron during summer although values of iron in the waters below the mixed layer were high in summer. For NBP0606, winter values of Fe in the surface waters over the shelf were ~ 4-5 nM, much higher than the values of 1 - 1.5 nM observed in summer during LMG0402. Deep eddy structures observed by the physical oceanography component led by Meng Zhou (ANT 04-44040) suggest that even in summer, the high iron values in deeper water may be mixed into the iron-poor ACC waters enhancing primary production in the Ona Basin and in the advective path defined by the drifters (Figures 2A, 14, 15; Measures et al. 2006; Zhou et al., 2006; Hewes et al. 2007; Hopkinson et al., 2007; Kahru et al. 2007). The higher biomass of phytoplankton results in enhanced rates of POC export as summarized in the report by Charette (ANT 04-43869). Data on net primary production (NPP) and POC export flux (EF) collected as part of this collaborative research project have been combined with similar data from diverse Southern Ocean projects (RACER, JGOFS, SOFEX, SOIREE) to form the basis for a synthesis that will be used in new satellite-based models for EF that is part of a global Southern Ocean carbon cycle modeling effort funded by NASA.

An important finding is that the higher Fe levels observed in winter, combined with the strong mixing of shelf-derived waters offshore by the Shackleton Jet that flows through the Shackleton Gap, will deliver a very significant supply during winter to the Southern Scotia Sea along the advective path of the drifters that remain bounded by the ACCPF and the ACCSB, along the mean path of the SACCF toward South Georgia. Thus, the entire Southern Scotia Sea may be primed with Fe during winter and poised to support the large open ocean blooms that we have discovered associated with intense eddy activity along the ACCSB (Figures 6, 14, and 15; Kahru et al. 2007). Using assumptions based on the rate of iron delivery from our study region during LMG0402 and NBP0606 extrapolated over a full year, Measures et al. (2006) report that the total supply of Fe to the Southern Scotia Sea from our study region near STR and the Elephant Island Shelf may be sufficient to supply Fe required to support up to 10% of all new production in the Southern Ocean. Future work should extend our study region to the shelves of South Orkney, South Sandwich and South Georgia Islands to develop a more comprehensive and quantitative understanding of interactions between the SACCF and ACCSB with shelf waters and delivery of Fe into the open Southern Ocean. Single regional surveys in each season will not be sufficient to understand interannual forcing that may play a significant role in the observed factor of 3 variations in POC export flux (EF) estimated by satellite time-series (Figure 1B). More detailed regional and multi-seasonal studies of how the fluid dynamics regulates shelf-iron delivery, and the consequences for plankton communities, are needed to create a foundation of knowledge as a baseline for future climate studies. In particular, it will be very important to understand how climate change will increase or decrease these shelf-derived iron delivery mechanisms and to quantify the role of shelf-derived iron in sustaining higher trophic levels that depend on oceanic plankton ecosystems. Such an understanding of climate change for the Scotia Sea will be impossible without future ship-based surveys that employ the intensive interdisciplinary approach that we have pioneered for this region.

## REFERENCES

Publication supported by NSF under these Collaborative Research awards for this interdisciplinary project:
Mitchell, et al. – ANT 04-44134
Charette –ANT 04-43869
Zhou – ANT 04-44040
Measures -ANT 04-43403

Allen, J. D., Bakker, J., Read, R., Pollard, Charette, M., Venables, H., Planquette, H., Morris, P., Sanders, R., Moore, M., Seeyave, S. 2006. An 'eddy-centric' bloom north of the Crozet Islands; sub-mesoscale entrainment of island nutrients or vertical diffusion? Challenger Conference for Marine Science, Oban, Scotland, September,

Allison, D. 2006, Identification of Relative Contributions of Particle Classes to Bulk Particulate Organic Carbon and Backscattering, EOS Trans. AGU, 87(36), Ocean Sci. Meet. Suppl., Abstract OS36I-03

Barbeau, K., Hopkinson, B.M., Reynolds, R., Wang, H., Selph, K., Measures, C., Hewes, C., Malfatti, F., Manganelli, M., Azam, F., Holm-Hansen, O., Mitchell, B. G. 2006. Phytoplankton iron stress across chlorophyll and dissovled-iron gradients in the Southern Drake Passage. Ocean Science Meeting Supplemental, Abstract OS33F-05.

Bourquin M., van Beek, P., Reyss, J-L., Souhaut, M., Charette, M., Jeandel, C. 2006. Radium isotopes to investigate the water mass pathways on the Kerguelen plateau (KEOPS project). Eos Trans. AGU, 87(52), Fall Meet. Suppl., Abstract OS21B-1584.

Bourquin, M., van Beek, P., Reyss, J. L., Souhaut, M., Jacquet, S., Dehairs, F., Charette, M., & Jeandel, C. 2007. Ra-226 activities and Ra-226/Ba ratios on the Kerguelen plateau, Southern Ocean (KEOPS project). Geochimica Et Cosmochimica Acta, 71(15): A115.

Bourquin M., van Beek, P., Reyss, J-L., Souhaut, M., Charette, M. and Jeandel, C. 2007. Testing methods to separate radium isotopes from seawater. Marine Chemistry, submitted.

Buck, K.N., Bruland, K.W., Measures, C.I., Barbeau, K.A. 2008. The biogeochemistry of iron and copper in Antarctic Peninsula shelf and Antarctic Circumpolar Current waters in the Southern Drake Passage. Ocean Sciences Meeting, (2008). Accepted.

Charette, M.A., Gonneea, M.E., Morris, P., Statham, P., Fones, G., Planquette, H., Salter, I., Naveira Garabato, A. 2007. Radium isotopes as tracers of iron sources fueling a Southern Ocean phytoplankton bloom. Deep-Sea Research II, in press.

Dorland, RD, Zhou, M, Circulation and Heat Fluxes during the Austral Fall in George VI Sound, Antarctic Peninsula. Deep Sea Research II, revised, 2007.

Dulaiova, H., Charette, M. A., Mitchell, B. G., Measures, C., Henderson, P., Supcharoen, R., Biller, D., 2007. Natural iron fertilization in the Southern Ocean: investigating horizontal iron transport and vertical carbon flux using radium isotopes and thorium-234. Winter ASLO Meeting, Santa Fe, NM.

Elipot, S., Gille, S. 2006. Wind Energy Input into Ekman Motions and Vertical Viscosity Estimates in the Southern Ocean. Eos Trans. AGU, 87(36), Ocean Sci. Meet. Suppl., Abstract OS46B-03.

Frants, M. 2006. Mixing Analysis of the Waters in the Shackleton Fracture Zone and the Ona Basin. AGU 2006 Fall Meeting, OS21C-1611.

Frants, M., Gille, S., Mitchell, B. G., Kahru, M. 2007. Geostrophic Transport and Biological Productivity in Southern Drake Passage. Ocean Surface Topography Science Team Meeting.

Hewes, C. D., Reiss, C.S., .Kahru, M., Mitchell, B.G., and Holm-Hansen, O. 2007. Control of phytoplankton biomass by dilution and mixed layer depth in the western Weddell-Scotia Confluence (WSC), Marine Ecology Progress Series. Submitted

Hiscock, M., Smith, Jr., W., Dinniman, M., Bidigare, R., Burke, H., Mitchell, B. G., Barber, R., The Influence of Modified Circumpolar Deep Water on Phytoplankton Photosynthesis in the Ross Sea. Deep-Sea Research. Submitted.

Hiscock, M., Lance, V., Apprill, A., Bidigare, R., Mitchell, B. G., Smith Jr., W., Barber, R. 2007 Photosynthetic maximum quantum yield increases are an essential component of the Southern Ocean phytoplankton response to iron. Proceedings of the National Academy of Sciences. Submitted

Holm-Hansen, O., Kahru, M., Hewes, C., 2005. Deep chlorophyll a maxima (DCMs) in pelagic Antarctic waters. II. Relation to bathymetric features and dissolved iron concentrations. Marine Ecology-Progress Series, vol. 297, p. 71.

Holm-Hansen, O., Azam, F., Barbeau, K., Gille, S., Hewes, C., Kahru, M., Mitchell, B. G. 2006. Plankton Community Structure and Iron Distribution in the Southern Drake Passage and Scotia Sea. Eos Trans. AGU, 87(36), Ocean. Sci. Meet. Suppl., Abstract OS35M-16.

Hopkinson, B., Mitchell, B. G., Reynolds, R. A., Wang, H., Selph, K., Measures, C., Hewes, C., Holm-Hansen, O., Barbeau, K. 2007. Iron limitation Across Chlorophyll Gradients in the Southern Drake Passage: Phytoplankton Responses to Iron Addition and Photosynthetic Indicators of Iron Stress. Limnology and Oceanography, p. 2540.

Kahru, M., Mitchell, B. G., Gille, S. T., Hewes, C. D. and Holm-Hansen, O. 2007 Eddies enhance biological production in the Weddell-Scotia Confluence of the Southern Ocean. Geophysical Research Letters, 34, vol. 24, p. L14603.

Kahru, M., Mitchell, B. 2006. Satellite Observations of Fronts in the Drake Passage: Implications for Carbon Eos TransCycling. AGU, 87(36), Ocean. Sci. Meet. Suppl., Abstract OS54D-01.

Malfatti, F., Manganelli, M., Azam, F. 2005. Bacterial response to carbon, nitrogen and iron in the Drake Passage, Antarctica: possible significance of microscale processes. ASLO, Santiago de Compostela, Spain, 19-24.

Measures, CI, Brown, MT, Selph, KE, Apprill, A, Zhou, M. 2006. The Influence of Shelf Processes in Delivering Dissolved Iron to the HNLC waters of the Drake Passage, Antarctica. Deep Sea Research I, in revision.

Mitchell, B.G., Wang, H., Reynolds, R., Delaney, N., Hewes, C., Holm-Hansen, O. 2006. Phytoplankton Community Structure and Photosynthesis Physiology Within a Natural Iron Gradient in the Southern Drake Passage. Eos Trans. AGU, 87(36), Ocean. Sci. Meet. Suppl., Abstract OS32A-05.

Mitchell B.G., Gille S.T., Hewes C.D., Kahru M., Holm-Hansen O., Reynolds R.A., Wang H.. Biological production in the Weddell-Scotia confluence of the Southern Ocean East of the Shackleton fracture zone. Continental Margins: Impacts of global, local and human forcings on biogeochemical cycles and ecosystems. 17 - 21 September 2007. Shanghai, China.

Moisan, T., Mitchell, B. G. 200 . Modeling Net Growth of Phaeocystis Antarctica Based on Physiological and Optical Responses to Light and Temperature. Limnology and Oceanography, submitted.

Planquette, H., Statham, P.J. Fones, G.R. Charette, M.A. Moore, M. Salter, I. Nédélec, F.H., Taylor, S.L., French, M., Baker, A.R., Mahowald, N., Jickells, T. D. 2007. Dissolved iron in the vicinity the Crozet Islands, Southern Ocean. Deep-Sea Research II, submitted.

Planquette, H., Statham, P.J., Fones, G.R., Charette, M.A. 2007. Dissolved iron in the vicinity of the Crozet Islands, Southern Ocean. EGU General Assembly, Vienna, Austria.

Selph, K. E., Apprill, A., Measures, C., Brown, M. 2005. Phytoplankton Distributions In The Shackleton Fraction Zone /Elephant Island Region Of The Drake Passage In February-March 2004. ASLO, Santiago de Compostela, Spain, 19-24 June 2005.

Selph, A., Measures, C., Brown, M., Apprill, A., Zhou, M. 2006. The Influence of Shelf Processes in Delivering Dissolved Iron to the HNLC waters of the Drake Passage, Antarctica. Eos Trans. AGU, 87(52), Fall Meet. Suppl., Abstract OS32B-01.

van Beek P., Bourquin, M., Reyss J-L., Souhaut M., Charette, M., Jeandel, C. 2007. Radium isotopes to investigate the water mass pathways on the Kerguelen plateau (KEOPS project). Deep-Sea Research II, in revision.

Wang, H., Allison, D. B., Reynolds, R. A., Kahru, M., Wieland, J., Mitchell, B. G. 2006. A Comparison of Particulate Absorption and Backscattering Properties between the Southern Ocean and California Current Eos Trans. AGU, 87(36), Ocean. Sci. Meet. Suppl, OS36C-02.

Zhou, M., Pearn, P., Zhu, Y., Dorland, R., 2006, The Western Boundary Current in the Bransfield Strait, Antarctica, Deep Sea Research I, 53:1244-1252.

Zhou, M, Zhu, Y, Dorland, RD, Dynamics of the current system in the southern Drake Passage. Deep Sea Research I, in revision, 2006.

Zhou, M, Zhu, Y, Dorland, R. 2006, Mesoscale Jets and Eddies in the Southern Drake Passage, EOS Trans. AGU, 87(36), Ocean Sci. Meet. Suppl.,Abstract OS12H-05.

Zhou, M, Tande, KS, Zhu, Y, Basedow, S., 2007. Productivity, trophic levels and size spectra in Northern Norwegian shelf regions, and comparison with the Southern Ocean. Deep Sea Research II, submitted.

## OTHER REFERENCES IN FINDINGS REPORT

Barbeau, K., Rue, E. L., Bruland, K. W., & Butler, A. 2001. Photochemical cycling of iron in the surface ocean mediated by microbial iron (III)-binding ligands. Nature, 413(6854): 409-413.

Barbeau, K., Rue, E. L., Trick, C. G., Bruland, K. T., & Butler, A. 2003. Photochemical reactivity of siderophores produced by marine heterotrophic bacteria and cyanobacteria based on characteristic Fe (III) binding groups. Limnology and Oceanography, 48(3): 1069-1078.

Behrenfeld, M. J., Bale, A. J., Kolber, Z. S., Aiken, J., & Falkowski, P. G. 1996. Confirmation of iron limitation of phytoplankton photosynthesis in the equatorial Pacific Ocean. Nature, 383: 508-511.

Biggs, D. C., Johnson, M. A., Bidigare, R. R., Guffy, J. D., & Holm-Hansen, O. 1982. Shipboard autoanalyzer studies of nutrient chemistry, 0-200 m, in the eastern Scotia Sea during FIBEX (January-March, 1981). College Station, Texas: Department of Oceanography Technical Report 88-11-T, Texas A & M.

Borer, P. M., Sulzberger, B., Reichard, P., & Kraemer, S. M. 2005. Effect of siderophores on the light-induced dissolution of colloidal iron(III) (hydr)oxides. Marine Chemistry, 93(2-4): 179-193.

Boyd, P. 2004. Ironing Out Algal Issues in the Southern Ocean. Science, 304(5669): 396-397.

Boyd, P. W., Watson, A. J., Law, C. S., Abraham, E. R., Trull, T., Murdoch, R., Bakker, D. C. E., Bowie, A. R., Buesseler, K. O., Chang, H., Charette, M., Croot, P., Downing, K., Frew, R., Gall, M., Hadfield, M., Hall, J., Harvey, M., Jameson, G., LaRoche, J., Liddicoat, M., Ling, R., Maldonado, M. T., Mckay, R. M., Nodder, S., Pickmere, S., Pridmore, R., Rintoul, S., Safi, K., Sutton, P., Strzepek, R., Tanneberger, K., Turner, S., Waite, A., & Zeldis, J.

2000. A mesoscale phytoplankton bloom in the polar Southern Ocean stimulated by iron fertilization. Nature, 407(6805): 695-702.
Boyd, P. W. 2002. The role of iron in the biogeochemistry of the Southern Ocean and equatorial Pacific: a comparison of in situ iron enrichments. Deep Sea Research Part II: Topical Studies in Oceanography, 49(9-10): 1803-1821.
Bruland, K. W., Rue, E. L., and Hunter, R. J. 2001. Analytical methods for the determination of concentrations and speciation of iron. Turner, D. R. Source pp.255-289; 2001; (The biogeochemistry of iron in seawater) John Wiley and Sons; Chichester.
Buesseler, K. O., Andrews, J. E., Pike, S. M., & Charette, M. A. 2004. The effects of iron fertilization on carbon sequestration in the Southern Ocean. Science, 304(5669): 414-417.
Buesseler, K. O., Barber, R. T., Dickson, M. L., Hiscock, M. R., Moore, J. K., & Sambrotto, R. 2003. The effect of marginal ice-edge dynamics on production and export in the Southern Ocean along 170[deg]W. Deep Sea Research Part II: Topical Studies in Oceanography, 50(3-4): 579-603.
Butler, A. 2005. Marine siderophores and microbial iron mobilization. Biometals, 18(4): 369-374.
Chalup, M. S. & Laws, E. A. 1990. A test of the assumptions and predictions of recent microalgal growth models using the marine phytoplankton *Pavlova lutheri*. Limnology and Oceanography, 35: 583-596.
Chisholm, S. W. & Morel, F. M. M. 1991. What controls phytoplankton production in nutrient-rich areas of the open sea? Limnology and Oceanography, 36(8): 1,507-1,511.
Church, M. J., Hutchins, D. A., & Ducklow, H. W. 2000. Limitation of bacterial growth by dissolved organic matter and iron in the Southern Ocean. Applied and Environmental Microbiology, 66(2): 455-466.
Coale, K. H., Johnson, K. S., Chavez, F. P., Buesseler, K. O., Barber, R. T., Brzezinski, M. A., Cochlan, W. P., Millero, F. J., Falkowski, P. G., Bauer, J. E., Wanninkhof, R. H., Kudela, R. M., Altabet, M. A., Hales, B. E., Takahashi, T., Landry, M. R., Bidigare, R. R., Wang, X. J., Chase, Z., Strutton, P. G., Friederich, G. E., Gorbunov, M. Y., Lance, V. P., Hilting, A. K., Hiscock, M. R., Demarest, M., Hiscock, W. T., Sullivan, K. F., Tanner, S. J., Gordon, R. M., Hunter, C. N., Elrod, V. A., Fitzwater, S. E., Jones, J. L., Tozzi, S., Koblizek, M., Roberts, A. E., Herndon, J., Brewster, J., Ladizinsky, N., Smith, G., Cooper, D., Timothy, D., Brown, S. L., Selph, K. E., Sheridan, C. C., Twining, B. S., & Johnson, Z. I. 2004. Southern ocean iron enrichment experiment: Carbon cycling in high- and low-Si waters. Science, 304(5669): 408-414.
Croot, P. L., Bowie, A. R., Frew, R. D., Maldonado, M. T., Hall, J. A., Safi, K. A., La Roche, J., Boyd, P. W., & Law, C. S. 2001. Retention of dissolved iron and Fe-II in an iron induced Southern Ocean phytoplankton bloom. Geophysical Research Letters, 28(18): 3425-3428.
Croot, P. L. & Johansson, M. 2000. Determination of iron speciation by cathodic stripping voltammetry in seawater using the competing ligand 2-(2-thiazolylazo)-p-cresol (TAC). Electroanalysis, 12(8): 565-576.
de Baar, H. J. W., Buma, A. G. J., Nolting, R. F., Cadee, G. C., Jacques, G., & Treguer, P. J. 1990. On iron limitation of the Southern Ocean: experimental observations in the Weddell and Scotia Seas. Marine Ecology- Progress Series, 65: 105-122.
De La Rocha, C. L., Hutchins, D. A., Brzezinski, M. A., & Zhang, Y. 2000. Effects of iron and zinc deficiency on elemental composition and silica production by diatoms. Marine Ecology - Progress Series, 195: 71-79.

Dubinsky, Z., Falkowski, P. G., & Wyman, K. 1986. Light harvesting and utilization by phytoplankton. Plant and Cell Physiology, 27(7): 1,335-1,349.
El-Sayed, S. Z. 1987. Biological production of Antarctic waters: Present paradoxes and emerging paradigms. In SCAR (Ed.), Antarctic aquatic biology, BIOMASS Scientific Series, Volume 7: 1-21. Cambridge, England: Scott Polar Research Institute.
Falkowski, P. G., Dubinsky, Z., & Wyman, K. 1985. Growth-irradiance relationships in phytoplankton. Limnology and Oceanography, 30: 311-321.
Fitzwater, S. E., Johnson, K. S., Gordon, R. M., Coale, K. H., & Smith, W. O. 2000. Trace metal concentrations in the Ross Sea and their relationship with nutrients and phytoplankton growth. Deep-Sea Research Part Ii-Topical Studies in Oceanography, 47(15-16): 3159-3179.
Fuhrman, J. A. 1999. Marine viruses and their biogeochemical and ecological effects. Nature, 399(6736): 541-548.
Geider, R. J., MacIntyre, H. L., & Kana, T. M. 1998. A dynamic regulatory model of phytoplanktonic acclimation to light, nutrients, and temperature. Limnology and Oceanography, 43(4): 679-694.
Greene, R. M., Kolber, Z. S., Swift, D. G., Tindale, N. W., & Falkowski, P. G. 1994. Physiological imitation of phytoplankton photosynthesis in the eastern equatorial Pacific determined from variability in the quantum yield of fluorescence. Limnology and Oceanography, 39: 1,061-1,074.
Hart, T. J. 1942. Phytoplankton periodicity in Antarctic surface waters. Discovery Reports, 21: 261-365.
Heywood, K. J., Garabato, A. C. N., Stevens, D. P., & Muench, R. D. 2004. On the fate of the Antarctic Slope Front and the origin of the Weddell Front. Journal of Geophysical Research-Oceans, 109(C6).
Hofmann, E. E., Klinck, J. M., Lascara, C. M., & Smith, D. A. 1996. Water Mass Distribution and Circulation West of the Antarctic Peninsula and including Bransfield Strait. Antarctic Research Series, 70: 61-80.
Holm-Hansen, O. 1985. Nutrient Cycles in Antarctic marine ecosystems. In Siegfried, W. R., Condy, P. R., & Laws, R. M. (Eds.), Antarctic nutrient cycles and food webs: 6-10. Berlin, Heidelberg: Springer-Verlag.
Holm-Hansen, O., Amos, A. F., Silva, N., Villafañe, V. E., & Helbling, E. W. 1994. *In situ* evidence for a nutrient limitation of phytoplankton growth in pelagic Antarctic waters. Antarctic Science, 6(3): 315-324.
Holm-Hansen, O. & Hewes, C. D. 2004. Deep chlorophyll-a maxima (DCMs) in Antarctic waters - I. Relationships between DCMs and the physical, chemical, and optical conditions in the upper water column. Polar Biology, 27(11): 699-710.
Hutchins, D. A. & Bruland, K. W. 1998. Iron-limited diatom growth and Si:N uptake ratios in a coastal upwelling regime. Nature, 393(6685): 561-564.
Hutchins, D. A., DiTullio, G. R., Zhang, Y., & Bruland, K. W. 1998. An iron limitation mosaic in the California upwelling regime. Limnology and Oceanography, 43(6): 1037-1054.
Kirchman, D. L., Meon, B., Cottrell, M. T., Hutchins, D. A., Weeks, D., & Bruland, K. W. 2000. Carbon versus iron limitation of bacterial growth in the California upwelling regime. Limnology and Oceanography, 45(8): 1,681-1,688.
Kolber, Z. S., Barber, R. T., Coale, K. H., Fitzwater, S. E., Greene, R. M., Johnson, K. E., Lindley, S. T., & Falkowski, P. G. 1994. Iron limitation of phytoplankton photosynthesis in the equatorial Pacific Ocean. Nature, 371: 145-149.

Laws, E. A. 2004. Export flux and stability as regulators of community composition in pelagic marine biological communities: Implications for regime shifts. Progress in Oceanography, 60(2-4): 343-353.

Laws, E. A., Falkowski, P. G., Smith, W. O., Jr., Ducklow, H. W., & McCarthy, J. J. 2000. Temperature effects on export production in the open ocean. Global Biogeochemical Cycles, 14(4): 1231-1246.

Lee, T., Barg, E., Lal, D., & Azam, F. 1993. Bacterial Scavenging of Th-234 in Surface Ocean Waters. Marine Ecology-Progress Series, 96(2): 109-116.

Loscher, B. M., de Baar, H. J. W., de Jong, J. T. M., Veth, C., & Dehairs, F. 1997. The distribution of Fe in the Antarctic Circumpolar Current. Deep-Sea Research, 44(1-2): 143-187.

Mackey, M. D., Mackey, D. J., Higgins, H. W., & Wright, S. W. 1996. CHEMTAX - A program for estimating class abundances from chemical markers: Application to HPLC measurements of phytoplankton. Marine Ecology-Progress Series, 144(1-3): 265-283.

Maldonado, M. T., Boyd, P. W., LaRoche, J., Strzepek, R., Waite, A., Bowie, A. R., Croot, P. L., Frew, R. D., & Price, N. M. 2001. Iron uptake and physiological response of phytoplankton during a mesoscale Southern Ocean iron enrichment. Limnology and Oceanography, 46(7): 1802-1808.

Maldonado, M. T., Strzepek, R. F., Sander, S., & Boyd, P. W. 2005. Acquisition of iron bound to strong organic complexes, with different Fe binding groups and photochemical reactivities, by plankton communities in Fe-limited subantarctic waters. Global Biogeochemical Cycles, 19(4).

Martin, J. H. 1990. Glacial-interglacial $CO_2$ change: the iron hypothesis. Paleoceanography, 5: 1-13.

Martin, J. H., Fitzwater, S. E., & Gordon, R. M. 1990a. Iron deficiency limits phytoplankton growth in Antarctic waters. Global Biogeochemical Cycles, 4: 5-12.

Martin, J. H., Gordon, R. M., & Fitzwater, S. E. 1990b. Iron in Antarctic waters. Nature, 345: 156-158.

Measures, C. I., Yuan, J., & Resing, J. A. 1995. Determination of iron in seawater by flow injection analysis using in-line pre concentration and spectrophotometric detection. Marine Chemistry, 50: 3-12.

Mitchell, B. G., Brody, E. A., Holm-Hansen, O., McClain, C., & Bishop, J. 1991. Light limitation of phytoplankton biomass and macronutrient utilization in the Southern Ocean. Limnology and Oceanography, 36(8): 1,662-1,677.

Mitchell, B. G. & Holm-Hansen, O. 1991. Observation and modeling of the Antarctic phytoplankton crop in relation to mixing depth. Deep-Sea Research I, 38: 981-1007.

Mitchell, B. G. & Kiefer, D. A. 1988. Chlorophyll *a* specific absorption and fluorescence excitation spectra for light-limited phytoplankton. Deep-Sea Research I, 35(5): 639-663.

Moisan, T. A. & Mitchell, B. G. 1999. Photophysiological acclimation of *Phaeocystis antarctica* Karsten under light limitation. Limnology and Oceanography, 44(2): 247-258.

Nolting, R. F., deBaar, H. J. W., Vanbennekom, A. J., & Masson, A. 1991. Cadmium, Copper and Iron in the Scotia Sea, Weddell Sea and Weddell Scotia Confluence (Antarctica). Marine Chemistry, 35(1-4): 219-243.

Olson, R. J., Sosik, H. M., Chekalyuk, A. M., & Shalapyonok, A. 2000. Effects of iron enrichment on phytoplankton in the Southern Ocean during late summer: Active fluorescence and flow cytometer analyses. Deep-Sea Research II, 47(15-16): 3,181-3,200.

Orsi, A. H., Whitworth, T., & Nowlin, W. D. 1995. On the meridional extent and fronts of the antarctic circumpolar current. Deep-Sea Research I-Oceanog.Res., 42(5): 641-673.

Resing, J. & Measures, C. I. 1994. Fluorometric determination of Al in seawater by FIA with in-line pre concentration. Analytical Chemistry, 66: 4,105-4,111.

Resing, J. A. & Mottl, M. J. 1992. Determination of manganese in seawater using flow injection analysis with on-line pre concentration and spectrophotometric detection. Analytical Chemistry, 64: 2,682-2,687.

Schlitzer, R. 2002. Carbon export fluxes in the Southern Ocean: results from inverse modeling and comparison with satellite-based estimates. Deep-Sea Research II, 49: 1623-1644.

Schodlok, M. P., Hellmer, H. H., & Beckmann, A. 2002. On the transport, variability and origin of dense water masses crossing the South Scotia Ridge. Deep Sea Research Part II: Topical Studies in Oceanography, 49(21): 4807-4825.

Sedwick, P. N. & DiTullio, G. R. 1997. Regulation of algal blooms in Antarctic shelf waters by the release of iron from melting sea ice. Geophysical Research Letters, 24(20): 2,515-2,518.

Sedwick, P. N., DiTullio, G. R., Hutchins, D. A., Boyd, P. W., Griffiths, F. B., Crossley, A. C., Trull, T. W., & Queguiner, B. 1999. Limitation of algal growth by iron deficiency in the Australian Subantarctic region. Geophysical Research Letters, 26(18): 2865-2868.

Smetacek, V. 2001. EisenEx: International Team Conducts Iron Experiments in Southern Ocean. U.S.JGOFS Newsletter, 11(1): 11-12.

Sosik, H. M. & Mitchell, B. G. 1991. Absorption, fluorescence and quantum yield for growth in nitrogen limited *Dunaliella tertiolecta*. Limnology and Oceanography, 36(5): 910-921.

Sosik, H. M. & Mitchell, B. G. 1994. Effects of temperature on growth, light absorption, and quantum yield in *Dunalliela tertiolecta* (chlorophyceae). Journal of .Phycology, 30: 833-840.

Strutton, P. G., Griffiths, F. B., Waters, R. L., Wright, S. W., and Bindoff, N. L. Primary productivity off the coast of East Antarctica (80-150E): January to March 1996. Deep-Sea Research. Part 2: Topical Studies in Oceanography 47[12/13], 2327-2362. 2000.

Takeda, S. 1998. Influence of iron availability on nutrient consumption ratio of diatoms in oceanic waters. Nature, 393(6687): 774-777.

Tomczak, M. Multi-Parameter Extension of Temperature/Salinity Diagram Techniques for the Analysis of Non-Isopycnal Mixing. 10[3], 147-171. 1981.

Tomczak, M. & Large, D. G. B. 1989. Optimum Multiparameter Analysis of Mixing in the Thermocline of the Eastern Indian-Ocean 2. Journal of Geophysical Research-Oceans, 94(C11): 16141-16149.

Wright, S. W., Thomas, D. P., Marchant, H. J., Higgins, H. W., Mackey, M. D., & Mackey, D. J. 1996. Analysis of phytoplankton of the Australian sector of the Southern Ocean: Comparisons of microscopy and size frequency data with interpretations of pigment HPLC data using the 'CHEMTAX' matrix factorisation program. Marine Ecology-Progress Series, 144(1-3): 285-298.